Spatial variability of organic matter molecular composition and elemental geochemistry in surface sediments of a small boreal Swedish lake

J. Tolu[1*], J. Rydberg[1], C. Meyer-Jacob[1], L. Gerber[2] and R. Bindler[1]

[1] *Department of Ecology and Environmental Science, Umeå University, SE-901 87 Umeå, Sweden*

[2] *Umeå Plant Science Center, Swedish University of Agricultural Sciences, Department of Forest Genetics and Plant Physiology, SE-901 83 Umeå, Sweden*

* Corresponding author. julietolu@hotmail.com

Abstract.

The composition of sediment organic matter (OM) exerts a strong control on biogeochemical processes in lakes, such as those involved in the fate of ~~for~~ carbon, nutrients and trace metals. While between-lake spatial variability of OM quality is increasingly investigated, we explored in this study how the molecular composition of sediment OM varies spatially within a single lake, and related this variability to physical parameters and elemental geochemistry. Surface sediment samples (0-10 cm) from 42 locations in Härsvatten – a small, boreal forest lake with a complex basin morphometry – were analyzed for OM molecular composition using pyrolysis gas chromatography-mass spectrometry, and for the contents of twenty-three major/trace elements and biogenic silica. 160 organic compounds belonging to different biochemical classes (e.g., carbohydrates, lignins, lipids) were identified. Close relationships were found between the spatial patterns of sediment OM molecular composition and elemental geochemistry. Differences in the source types of OM (i.e. terrestrial, aquatic plant and algal OM) were linked to the individual basin morphometries and chemical status of the lake. The variability in OM molecular composition was further driven by the degradation status of these different source pools, which appeared to be related to sedimentary physico-chemical parameters (e.g., redox conditions) and to the molecular structure of the organic compounds. Given the high spatial variation in OM molecular composition within Härsvatten and its close relationship with elemental geochemistry, the potential for large spatial variability across lakes should be considered when studying biogeochemical processes involved in the cycling of carbon, nutrients and trace elements or when assessing lake budgets.

Keywords.

Lake sediment; spatial variability; organic matter; molecular composition; Py-GC/MS; elemental geochemistry

1. Introduction

In lake basins a wide range of factors are known to influence the transport and fate of sedimentary material, such as the location of inlet streams, catchment topography, land-use patterns, fetch, basin morphometry and sediment focusing. Sediment focusing results from a combination of factors such as wind and wave action, basin slope and the settling velocity of different particle sizes, which all contribute to the redistribution of light, fine-grained material rich in clays, organic matter (OM) and associated trace elements from shallower to deeper waters (Blais and Kalff, 1995; Ostrovsky and Yacobi, 1999). While sediment focusing is important, catchment characteristics and lake morphometry can be complex and exert a primary influence on spatial patterns in sediment geochemistry, such as in relation to land use in near-shore areas (Dunn et al., 2008; Vogel et al., 2010; Sarkar et al., 2014), complex lake/basin morphometries (Bindler et al., 2001; Rydberg et al., 2012) or river inflows (Kumke et al., 2005). The presence of macrophytes or wind-induced water currents have also been shown to affect the spatial distribution of e.g., lead (Pb), phosphorus (P) and OM (Benoy and Kalff, 1999; Bindler et al. 2001).

Because trace metals and nutrients are primarily associated with – or are part of – OM, studies focusing on the spatial patterns of metal or nutrient accumulation typically include an analysis of the OM content. The two standard approaches to determine sediment OM content are the analysis of loss-on-ignition (LOI; Ball, 1964; Santisteban et al., 2004) or the analysis of elemental carbon (C). However, either approach inherently treats OM as a homogeneous sediment component. Recent studies interested in the role of sediments as a long-term C sink have likewise mainly treated OM and C as a homogeneous component (e.g., Sobek et al., 2003; Tranvik et al., 2009; Heathcote et al., 2015). Even if this approach is rational from a global perspective of calculating C budgets, treating OM as a homogeneous component is overly simplistic from the perspective of developing insights into the biogeochemical behavior of OM and its influence on C, nutrients and

52 trace metals cycling, and does not take full advantage of the information provided by differences in
53 the OM quality.

54 In boreal lakes the sediment composition is often dominated by OM, typically ranging from 20
55 to 60 % on a dry weight basis, followed by biogenic silica (bSi), which may account for as much as
56 45 % of the sediment dry weight (Meyer-Jacob et al., 2014). The remaining sediment mainly
57 consists of detrital mineral matter and possibly authigenic minerals. Lake OM is an extremely
58 heterogeneous and complex mixture of molecules that are derived from plant, animal, fungal and
59 bacterial residues, and which are either transported into the lake from the surrounding catchment
60 (allochthonous) or produced within the lake (autochthonous). Furthermore, these organic
61 compounds may undergo transformations within the water column and the sediment through both
62 biotic and abiotic processes. Although there have been a few studies where the spatial complexity in
63 OM quality within a lake basin has been assessed using infrared spectroscopy, which yields
64 qualitative information on variations in OM quality (Korsman et al., 1999; Rydberg et al., 2012), or
65 using quantitative analyses of photopigments and lipids (Ostrovsky and Yacobi, 1999; Trolle et al.,
66 2009; Vogel et al., 2010; Sarkar et al., 2014), little work has been done to detail how the molecular
67 composition of the sediment OM matrix, considering a large number of organic biochemical classes
68 and compounds, varies spatially within a lake.

69 To characterize OM composition at the molecular level, the most commonly used methods are
70 based on liquid or gas chromatography (LC or GC) coupled to fluorescence or mass spectrometry
71 (MS) detection. These methods provide quantitative data on original organic compounds found in
72 the analyzed samples, including highly specific biomarkers of, e.g., OM sources, and have been
73 successfully employed to study OM composition and reactivity in environmental matrices as well
74 as to reconstruct environmental changes (e.g., changes in vegetation, algal productivity) from peat
75 or sediment cores. However, the associated sample preparation procedures, i.e.
76 extraction/hydrolysis and derivatization, are fastidious and specific to the different biochemical
77 classes of organic compounds such as carbohydrates, proteins/amino acids, lipids, chlorophylls and

lignins (e.g., Wakeham et al., 1997; Dauwe and Middelburg, 1998; Tesi et al., 2012). Moreover, sample masses > 10 mg are required. Hence, studies where different OM biochemical classes are targeted using these wet chemical extraction and GC/LC-MS methods are very scarce. However, efforts in characterizing the whole OM composition at the molecular level can bring important insights because the different biochemical classes of OM do not always include specific biomarkers for the different existing sources of OM (e.g., terrestrial plants, macrophytes, higher plants, mosses, algae, bacteria). For example, lignin compounds are only specific of higher plants (Meyer and Ishiwatari, 1997) and proteins/amino-acids mainly provide biomarkers for bacteria and planktonic production (Bianchi and Canuel, 2011). Moreover, the different biochemical classes of OM do not present the same reactivity; for example, proteins/amino-acids and neutral carbohydrates have been shown to be among the most reactive organic molecules (e.g., Fichez, 1991; Dauwe and Middelburg, 1998; Amon and Fitznar, 2001; Tesi et al., 2012). Advanced ultrahigh-resolution MS techniques, i.e. Fourier transformed-ion cyclotron resonance-mass spectrometry (FT-ICR-MS) or Linear trap Quadruple-Orbitrap-MS enable the determination of a large number of organic molecular formulas, belonging to the different biochemical classes of OM in liquid samples (> 1000; e.g., Hawkes et al., 2016). These method have been successfully used to link variability in the molecular composition of dissolved OM (DOM), also called DOM chemodiversity, with different factors and/or processes of environmental ecosystems, such as climate, hydrology and OM degradation in boreal lakes (Kellerman et al., 2014; Kellerman et al., 2015) or optical properties and DOM photo-chemical alterations in wetland and seawater (Stubbins and Dittmar, 2015; Wagner et al., 2015). But, in addition to the limited access to these advanced MS techniques due to instrumental costs, extraction/hydrolysis steps are required when studying solid samples, which make these methods also specific to the different biochemical classes of organic compounds.

To study the variability of OM composition in sediments, pyrolysis-gas chromatography – mass spectrometry (Py-GC/MS) is a good compromise between the quantitative LC/GC-MS or the high-resolution MS methods that target specific compounds and the qualitative, non-molecular

104 information provided by high-throughput techniques such as infrared spectroscopy or 'RockEval'
105 pyrolysis. The sample preparation for Py-GC/MS analysis requires no complex sample preparation
106 but yields semi-quantitative data on >100 organic compounds that are chemical fingerprints of the
107 different OM biochemical classes, which include specific biomarkers for OM sources and OM
108 degradation status (Faix et al., 1990; Faix et al., 1991; Peulvé et al., 1996; Nierop and Buurman,
109 1998; Schulten and Gleixner, 1999; Lehtonen et al., 2000; Nguyen et al., 2003; Page, 2003;
110 Buurman et al., 2005; Fabbri et al., 2005; Kaal et al., 2007;Vancampenhout et al., 2008;
111 Schellekens et al., 2009 ;Carr et al., 2010; Buurman and Roscoe, 2011; De La Rosa et al., 2011 ;
112 Mcclymont et al., 2011; Micić et al., 2011; Stewart, 2012). Recently, we developed a method where
113 Py-GC/MS is combined to a data processing pipeline in order to speed up the peak identification
114 and integration that are otherwise very time-consuming (Tolu et al., 2015).

115 In the present study, we apply ~~a~~ our newly optimized Py-GC/MS method to characterize the
116 molecular composition of natural OM in surface sediments (0-10 cm) from 42 locations within the
117 lake basin of Härsvatten, a small boreal forest lake in southwestern Sweden that was previously
118 studied for the spatial distribution of Pb and OM contents (Bindler et al., 2001). Our objective here
119 was to comprehensively investigate how the molecular composition of sediment OM varies
120 spatially across a lake with several basins. Our specific research questions were: (i) what are the
121 spatial patterns within a single lake for various organic biochemical classes and compounds?; (ii)
122 how does the spatial pattern of the OM molecular composition relate to physical parameters (i.e.,
123 bulk density and water depth) and elemental, inorganic geochemistry of the sediment material?; (iii)
124 which factors or processes (e.g., provenance, transport pathway, mineralization) appear to explain
125 the in-lake spatial variability of the OM molecular composition?

2. Materials and Methods

2.1 Study site and samples

Härsvatten is a boreal forest lake located in southwestern Sweden (58°02' N 12°03' E) in the Svartedalen nature reserve. This culturally acidified, clear-water, oligotrophic and fishless lake has been intensively monitored since the 1980's (national database, Dept. of aquatic sciences and assessment, Swedish university of agricultural sciences, Uppsala, Sweden; www.slu.se), during which time the pH has ranged from 4.2-4.5 in 1983–1987 to 4.7-5.6 in 2010–2014. The lake is dimictic with a thermal stratification between 10 and 15 m depth in the summer. Approximately 80 % of the lake bottom is within the epilimnion. The surface areas of the lake and its catchment are 0.186 and 2.03 km^2, respectively. The catchment is characterized by an uninhabited, coniferous-dominated forest (*Picea abies* Karst. and *Pinus sylvestris* L.), which extends to the rocky shoreline. The bedrock consists of slow-weathering granites and gneisses that are covered by thin and poorly developed podsolic soils.

The basin of Härsvatten can be divided into four general areas (Bindler et al., 2001): 1) the main south basin, which represents about half of the lake area (sample sites S1–24; maximum depth, 24.3 m) and includes the lake's small outlet stream; 2) a north basin (sample sites N1–11; maximum depth, 12 m), which includes a small inlet stream draining from the headwater lake Måkevatten that enters Härsvatten through a small wetland; 3) an east basin, which has a maximum depth of nearly 10 m (sample sites E1–6) and is separated from the main north–south axis of the lake by a series of islands and shallow sills (<3 m water depth); and 4) a generally shallow (<3 m water depth) central area separating the north/east and south basins (sample sites M1–6).

In total, we analyzed 44 surface sediment (0–10 cm) samples that were collected in winter 1997–1998 (Fig. 1) for a study of Pb and SCP (Bindler et al., 2001). These samples were collected as follow: short sediment cores (0-25 cm) were taken with a gravity corer from the ice-covered lake

in winter 1997 and 1998, and were sectioned into an upper sample (0-10 cm) and a lower sample (10-25 cm; not studied here) on-site. In the laboratory, the samples were weighed, freeze-dried, and reweighed to determine the water content and dry mass of the sediment. The freeze-dried samples have been stored in plastic containers within closed boxes shielded from light and at room temperature since winter 1997-1998. Before further analysis in this study, the samples were finely ground at 30 Hz for 3 min using a stainless steel Retsch swing mill.

2.2 Major and trace elements concentrations

The concentrations of major (Na, Mg, Al, Si, K, Ca, P, S, Mn, Fe) and trace elements (Sc, Ti, V, As, Br, Y, Zr, Ni, Cu, Zn, Sr, Pb) were determined using a wavelength dispersive X-ray fluorescence spectrometer (WD-XRF; Bruker S8 Tiger) and a measurement method developed for powdered sediment samples (Rydberg, 2014). Accuracy was assessed using sample replicates, which were within ±10 % for all elements.

Total mercury (Hg) concentrations were determined using thermal desorption atomic absorption spectrometry (Milestone DMA80) with the calibration curves based on analyses of different masses of four certified reference materials (CRMs). Analytical quality was controlled using an additional CRM and replicate samples included with about every ten samples. The CRM was within the certified range, and replicate samples were within ±10% for Hg concentrations <30 μg kg^{-1} and within ±5% for concentrations ≥30 μg kg^{-1}.

We also included the OM content (in % dry mass), determined as loss-on-ignition (LOI) after heating dried samples at 550ºC for 4 h in the earlier study of Bindler et al. (2001).

2.3 Biogenic silica concentrations

Biogenic silica (bSi) was determined by Fourier transform infrared (FTIR) spectroscopy following the approach described in Meyer-Jacob et al. (2014). In brief, sediment samples were mixed with potassium bromide (0.011 g sample and 0.5 g KBr) prior to analysis with a Bruker Vertex 70 equipped with a HTS-XT accessory unit (multisampler). The recorded FTIR spectral information were used to determine the bSi concentrations employing a PLSR calibration based on analyses of synthetic sediment mixtures with defined bSi content ranging from 0 to 100 %.

We calculated the mineral Si fraction ($Si_{mineral}$) from the difference between the total Si concentration determined by WD-XRF (Sect. 2.2) and the bSi concentration.

2.4 Organic matter molecular composition

The molecular composition of OM was determined by pyrolysis-gas chromatography-mass spectrometry (Py-GC/MS) following the method developed by Tolu et al. (2015). In brief, 200 ± 10 µg sediment was pyrolyzed in a FrontierLabs PY-2020iD oven (450 °C) connected to an Agilent 7890A-5975C GC/MS system. Peak integration was done using a data processing pipeline under the 'R' computational environment, and peak identification was made using the software 'NIST MS Search 2' containing the library 'NIST/EPA/NIH 2011' and additional spectra from published studies.

In the sediments of Härsvatten, 162 Py-products were identified, and peak areas were normalized by setting the total identified peak area for each sample to 100 %. A detailed list of the 160 identified organic compounds with information on their molecular mass and structure and on their reference mass spectra and calculated or reference retention index values is provided in the supplementary information (Table S1). Although the pyrolysis temperature we employed, i.e. 450°C as used in plant science (e.g., Faix et al., 1990; Faix et al., 1991), is different from the

pyrolysis temperature most commonly used in previous studies analyzing soils, sediments and peat records (i.e. >600°C), our list is highly similar to published lists of identified pyrolytic organic compounds both in terms of the organic compounds and of their classification into 13 OM classes (Faix et al., 1990; Faix et al., 1991; Peulvé et al., 1996; Nierop and Buurman, 1998; Schulten and Gleixner, 1999; Lehtonen et al., 2000; Nguyen et al., 2003; Page, 2003; Buurman et al., 2005; Fabbri et al., 2005; Kaal et al., 2007;Vancampenhout et al., 2008; Schellekens et al., 2009 ;Carr et al., 2010; Buurman and Roscoe, 2011; De La Rosa et al., 2011 ; Mcclymont et al., 2011; Micić et al., 2011; Stewart, 2012). We used a pyrolysis temperature of 450°C because during our methodological development for lake sediments, we showed that, when using sub-mg sample mass, a pyrolysis performed at this temperature enable to avoid complete degradation of some specific biomarkers of OM sources and/or degradation status (e.g., syringol lignin oligomers, Py products of polysaccharides and/or cellulose) as compared to 650 °C (Tolu et al., 2015).

2.5 Statistical analysis

We performed all statistical analyses using SPSS software package PASW, version 22.0. Two separate principal component analyses (PCA) were performed, one for the elemental geochemistry (i.e., dry bulk density (B.D.) and contents of OM (LOI), major/trace elements and bSi) and the other for the OM molecular composition. Prior to the PCA, all data were converted to Z-scores (average = 0, variance = 1). Principal components (PCs) with eigenvalues > 1 were extracted using a Varimax rotated solution. Factor loadings were calculated as regression coefficients, which is analogous to *r* in Pearson correlations. For convenience the loadings are reported as percentage of variance explained, i.e., as squared loadings. For all PCs, variables with squared loadings <0.15 are not discussed with respect to that PC. Others variables, e.g., water depth (W.D.) or ratios between elements, were included passively in the PC-loadings plots by using bi-variate correlation coefficients between these variables and the PC-scores of each PC. Hierarchical agglomerative

cluster analysis (CA) was performed for the elemental geochemistry and the OM molecular composition datasets using Wards linkages (Ward, 1963) based on squared Euclidean distances. The PC-scores from the PCAs were used instead of the original data in order to eliminate the effects of autocorrelation in the dataset.

3. Results and discussion

3.1. Sediment elemental geochemistry

3.1.1 General description and trends

Summary statistics of the elemental geochemical properties of the surface sediments from Härsvatten are presented in Table 1 and the detailed data are given in Table S2 in SI. The sediments from sites M4 and S15 are two outliers because they have a B.D., bSi, OM and elemental contents (e.g., Na, Mg, Al, K) that deviated by more than four standard deviations from the average values of all analyzed sediment samples (Table 1). Because these sediment samples are too coarse (predominantly sand) for Py-GC/MS analysis according to our method based on 200 ± 20 µg analyzed sample mass, they are excluded from the statistical analyses and discussion. Even when excluding these two sites, the elemental geochemical parameters vary considerably across the lake basin, with Hg, Fe, Co and Mn contents illustrating the greatest variabilities (i.e., coefficient of variation, CVs >60%) and Al, Br, K, Ti, V, Ni, Mg and Ca contents showing the lowest variabilities (CVs: 17-25%; Table 1). For most of geochemical properties, the average to median ratios are approximatively 1.0, indicating no extreme values. Slightly higher values were, however, observed for P, Fe, As and Co contents (1.2-1.3), and Mn content is associated with extremely large values outside the population distribution (average:median = 4.1).

The lowest B.D. is observed among the three deepest sampling locations (23.5-24.5 m) in the main south basin, where we also find the lowest bSi content and the highest contents in organically bound elements including S, Br, P and certain trace metals, i.e. Cu, Ni, Hg and Zn. These sediments have high OM content (> 50%), but the highest [OM] (57-58%) are observed among isolated sites that are located close to the shoreline (N1-2, E3, S5, S23; 3.1-7.4) and which also include the lowest [Al], [P], [K], [$Si_{inorganic}$], [V] and [Zr]. The highest B.D. and the lowest [OM], [S], [Br], [Cu], [Ni], [Hg] and [Zn] are observed among the shallow sites (1.8-2.5 m) located between the north and east basins and between the larger north and south basins (i.e., sites N10, M1, M5-6), which also contain the highest [bSi], [Sr], [Al], [Y], [Mn] and [Co]. The sediments located at intermediate water depth (9-20 m) in the main south basin (S4, S9, S11, S13-14, S17, S19, S22) are associated with the highest [Fe], [As], [K], [Mg], [Na], [Ti] and [Zr], while among the shallower sites of the south basin we find the highest [$Si_{inorganic}$]. The lowest [Fe], [As], [Co] and [Y] are observed among the sediments of the east basin, and the sediments of the north basin include the lowest [Mn], [Ca], [K], [Mg], [Na], [Sr] and [Zr]. To identify more accurately the most significant relationships existing between the different elemental geochemical properties and o explore more precisely their spatial distribution, the results of PCA and cluster analyses are further presented and discussed.

3.1.2. Principal components of the elemental geochemistry

For the elemental geochemistry dataset, five principal components were extracted. We present only the first four PCs, which together explain 74 % of the total variance (PC1-4_{geo}; Fig. 2) because no reasonable interpretation could be made for $PC5_{geo}$ (10 % of the total variance; Fig. S1 in SI). $PC1_{geo}$ captures 25 % of the total variance and separates bSi and B.D. (negative loadings) from OM, S, Cu, Hg, Ni, Zn and, to a lesser extent, As and Pb (positive loadings; Fig.2a). This means that bSi and B.D. are significantly positively correlated, and both are significantly negatively correlated to

277 OM, S, Cu, Hg, Ni, Zn and, to a lesser extent, As and Pb. If those parameters do not have
278 significant loadings on PC2-5, it means there are not significantly correlated with the parameters
279 found on PC2-5, the PCs being orthogonal to each other. The negative loadings are interpreted as
280 reflecting a bSi-rich fraction, while positive loadings indicate an organic-rich fraction that is
281 enriched in organophilic trace metals (Lidman et al., 2014). For $PC2_{geo}$, which captures 21 % of the
282 total variance, $Si_{inorganic}$, K, Na, Mg, Zr and Ti have positive loadings, while no element is
283 significantly negatively correlated to $PC2_{geo}$ (Fig. 2a). High $PC2_{geo}$ scores likely represent samples
284 that are richer in silicate minerals such as quartz and clays (Koinig et al., 2003; Taboada et al.,
285 2006).

286 Positive loadings on $PC3_{geo}$, which explains 16 % of the total variance, are found for Al and Fe
287 along with As, P and Y (Fig. 2b). Compared to elements such as Mg, Na and K that are mostly
288 confined to the silicate fraction of sediments, Fe and Al may reflect both detrital material and dissolved
289 or amorphous phases. However, the fact that As and P contents as well as the Fe:Al ratio plot together
290 with Fe and Al contents on the positive side of $PC3_{geo}$, but not with the S content, strongly suggest that
291 sediments with high $PC3_{geo}$ scores are associated with higher contents of Fe and Al (oxy)hydroxides,
292 which are known to strongly bind both As and P (Mucci et al., 2000; Plant et al., 2005; Zhu et al.,
293 2013). $PC4_{geo}$ captures 12 % of the total variance and separates Mn, Co, Pb and to a lesser extent Fe
294 (positive loadings) from OM and Br (negative loadings; Fig. 2b). Although Mn, like Fe and Al, is
295 not confined to a specific mineral phases and can reflect both detrital or dissolved and amorphous
296 phases, the positive loadings are interpreted as reflecting Mn (oxy)hydroxides, which bind Pb,
297 especially when they contain cobalt (Co) (Yin et al., 2011). This interpretation is supported by the
298 positive loadings on $PC4_{geo}$ of the ratio Mn:Fe, often used as a paleolimnological proxy for bottom
299 water oxygenation (Naeher et al., 2013). The negative loadings could indicate a terrestrial OM
300 fraction that is rich in Br (Leri and Myneni, 2012).

3.1.3 Cluster analysis of the elemental geochemistry

For the cluster analysis of the elemental geochemistry dataset, we selected a solution of six clusters ($cluster_{geo}$ 1–6; Fig. 1c). The cluster averages and standard deviations of each physical and geochemical variable are given in Table S3 in SI where they are compared to the averages values of all analyzed sediment samples, which are referred to hereafter as 'whole-lake average', and Table 3 provides the cluster averages for a selection of geochemical parameters.

In the south basin, the sediments found at shallower water depth ($cluster_{geo}$ 6; n=10) have a higher B.D., are richer in bSi (negative scores on $PC1_{geo}$; Fig. 2a) and have lower than whole-lake average trace metal concentrations (Table 1). In contrast, the sediments from the deeper sites ($cluster_{geo}$ 5; n=3) have the lowest B.D. and lowest bSi content (Table 1), and are enriched in OM and trace metals (positive scores on $PC1_{geo}$; Fig. 2a). The sediments found at intermediate water depths ($cluster_{geo}$ 2; n=8) have positive scores on $PC2_{geo}$ (Fig. 2a), and they have an OM content within 10% of whole-lake average while trace metal concentrations are above 10% of whole-lake averages (Table 1). The south basin as a whole has higher P concentrations than the northern, eastern and center areas, and in both intermediate and deeper sites, the sediments are rich in Fe and As (positive scores on $PC3_{geo}$; Fig. 2b and Table 1).

The sediments found at shallow water depth between the north and east basins and in the central area ($cluster_{geo}$ 3; n=4) have the highest B.D. and are the most enriched in both bSi (negative score on $PC1_{geo}$; Fig. 2a) and Mn and Fe (oxy)hydroxides (positive score on $PC4_{geo}$; Fig. 2b). A small number of shallow, near-shore sampling locations ($cluster_{geo}$ 4; n=4) have higher OM concentrations than the whole-lake average, and are enriched in S and trace metals (positive scores on $PC1_{geo}$; Fig. 2a and Table 1).

3.2 Sediment organic matter molecular composition

3.2.1 General description and trends

The Py-products identified in the surface sediments of Härsvatten were classified into 13 OM classes, i.e., carbohydrates, N-compounds, chitin-derived Py products, phenols, lignins, chlorophylls, *n*-alkenes, *n*-alkanes, alkan-2-ones, steroids, tocopherol, hopanoids, and (poly)aromatics, in agreement with previous studies using Py-GC/MS for different environmental matrices such as soil, sediment, peat cores, plants or algae (Faix et al., 1990; Faix et al., 1991; Peulvé et al., 1996; Nierop and Buurman, 1998; Schulten and Gleixner, 1999; Lehtonen et al., 2000; Nguyen et al., 2003; Page, 2003; Buurman et al., 2005; Fabbri et al., 2005; Kaal et al., 2007;Vancampenhout et al., 2008; Schellekens et al., 2009 ;Carr et al., 2010; Buurman and Roscoe, 2011; De La Rosa et al., 2011 ; Mcclymont et al., 2011; Micić et al., 2011; Stewart, 2012). For the sake of making the presentation of the data and the associated discussion more constrained (and avoid over-interpreting individual compounds), the 160 identified organic compounds were reduced to 41 groups of compounds as described in Table 2. This grouping is based on the similarities in the molecular structure within the OM classes, and preliminary principal components analyses have shown that the compounds within each of our 41 groups are highly positively correlated and thus present the same trends in this study (data not shown). As an example, the 20 identified carbohydrate compounds, previously demonstrated to derive from pyrolysis of polysaccharides (Faix et al., 1991), have been separated into 6 groups based on the number of C in the heterocycles of these compounds and on their side-chain functional groups. Thus, the heterocycle of "furan" and "furanone" compounds contains 4 C and 1 oxygen (O) atoms, and the side-chain are either aliphatic ((alkyl)furans and (alkyl)furanones) or contains an oxygenated functional group (hydroxy- or carboxy-furans and furanones). While the heterocycle of "pyran" compounds has 5 C and 1 O, the one of dianhydrohamnose, levoglucosenone and levosugars consists in 6 C and 1 O, but the

levosugars contain three hydroxyl functional groups whereas dianhydrorhamnose contains 2 hydroxyl groups and levoglucosenone have a carbonyl group.

Summary statistics of these 41 groups of organic compounds are presented in Table 2 and the detailed data are given in Table S4 in SI. The coefficients of variation for the abundances of the different organic compound groups range from 15 to 106 % with an average of 38 ± 20 %, showing a remarkable in-lake variability of OM molecular composition (Table 2). For most of the organic compound groups, the average to median ratios are approximatively 1.0, indicating no extreme values. However, slightly higher values (1.2-1.8) are observed for organic compounds derived from higher plants and mosses, i.e. levosugars, lignin oligomers (syringols and guaiacols), *n*-alkanes C25-35, alkan-2-ones C23-31 and tocopherols.

Most of the N-compounds, which usually derive more from algae than from higher plants and mosses (Bianchi and Canuel, 2011), have the highest abundances among the three deepest sampling locations (23.5-24.5 m) in the main south basin (S12, S18 and S24). Pyrolytic compounds containing an acetamide functional group previously shown to be a good indicator of the presence of chitin from micro-organisms exoskeletons in biological and geological samples (Gupta et al., 2007), phytadienes (i.e., pyrolytic products of chlorophylls; Nguyen et al., 2003), short-chain alkan-2-ones (2K C13-17) and steroids present also the highest abundances among the three deepest sampling locations. In contrast, most of the carbohydrates, which usually derive mostly from higher plants and mosses (Bianchi and Canuel, 2011), have the highest abundances among the sediments situated close to the shoreline (N1-2, E3, S5, S23) such as for the abundances of phenols, guaiacyl- and syringyl-lignin oligomers, long-chain *n*-alkenes (C27-28:1) and diketodipyrrole (N-compounds), all specific of higher plants and/or mosses OM (Meyers and Ishiwatari, 1993; Schellekens et al., 2009). The highest abundances of long-chain *n*-alkanes (C23-26:0 and C27-35:0) and mid-chain *n*-alkanes (C17-22:0) are, however, observed for the shallower sites (<2 m) situated between the larger north and south basins (sites M5-6).

375 Among the shallow sites (2.5-3.0 m) located between the north and east basin (N10, M1) and
376 the shallow and intermediate water depth (4-20 m) sites of the south basin (S1-4, S6-11, S13-17,
377 S19-22), we find the highest abundances of degradation products of carbohydrates (i.e.,
378 (alkyl)furans & furanones and hydroxyl- or carboxy-furans & furanones), of proteins, amino-acids
379 and/or chlorophylls (i.e., pyridines_O, (alkykl)pyrroles, pyrroles_O, pyrroledione &
380 pyrrolidinedione, pristenes) and of cell wall lipids (i.e., short-chain *n*-alkenes and *n*-alkanes – C9-
381 16:1 and C13-16:0) as well as the highest abundances of (poly)aromatic compounds indicative of
382 highly degraded OM (Schellekens et al., 2009; Buurman and Roscoe, 2011). The lowest
383 abundances of the (poly)aromatic and certain aliphatic compounds (i.e. *n*-alkenes C17-22 and C27-
384 28, *n*-alkanes C13-16 and alkan-2-ones C13-17) are observed among the sediments located close to
385 the shoreline (N1-2, E3, S5, S23), while the two shallow sites situated between the larger north and
386 south basins (M5-6) present the lowest abundances for all other organic compounds. To identify
387 more accurately the most significant relationships existing between the different organic
388 compounds groups and to explore more precisely their spatial distribution, the results of PCA and
389 cluster analyses are further presented and discussed.
390
391 *3.2.2 Principal components of OM molecular composition*
392
393 For the OM molecular composition dataset, six principal components ($PC1\text{-}6_{OM}$) were
394 extracted, which explain 85 % of the total variance (Fig. 3). $PC1_{OM}$, which captures 30 % of the
395 total variance, separates organic compounds that are produced during OM degradation (positive
396 loadings), from molecules of higher plant or moss origin including those that are readily
397 mineralized (negative loadings; Fig. 3a). Compounds with positive loadings include i)
398 (poly)aromatics (i.e., benzene, acetylbenzene, benzaldehyde, alkylbenzenes C2-9 and
399 polyaromatics); and ii) degradation products of carbohydrates ((alkyl)furans & furanones;
400 Schellekens et al., 2009), proteins, amino acids and/or chlorophylls (aromatic N, (alkyl)pyridines

401 and (alkyl)pyrroles; Jokic et al., 2004; Sinninghe Damsté et al., 1992) and cell wall lipids (short-
402 chain *n*-alkanes – C13-16:0 –-, *n*-alkenes – C9-16:1 – and alkan-2-ones – 2K C13-17 –;
403 Schellekens et al., 2009). The molecules of plant origin with negative loadings are syringol and
404 guaiacol lignin oligomers that are specific for vascular plants, long-chain *n*-alkenes (C23-26:1 and
405 C27-28:1) deriving from cell wall lipids of higher plants and/or mosses (Meyers and Ishiwatari,
406 1993) and long-chain alkan-2-ones (2K C23-31). Alkan-2-ones C23-31 may arise with degradative
407 oxidation of *n*-alkanes/*n*-alkenes (Zheng et al., 2011) or are good biomarkers for mosses such as
408 *Sphagnum* (2K C23-25) and for aquatic higher plants (2K C27-31) (Baas et al., 2000; Hernandez et
409 al., 2001; Nichols and Huang, 2007). Furthermore, anhydrosugars, Py-products of fresh, high-
410 molecular weight carbohydrates and cellulose from higher plants and mosses (never reported in Py-
411 chromatograms of algae or arthropods; Marbot, 1997; Nguyen et al., 2003; Valdes et al., 2013), and
412 the ratio Anhydrosugars: (alkyl)furans & furanones, a proxy for plant OM freshness (Schellekens et
413 al., 2009), have also negative loadings on $PC1_{OM}$ (Fig. 3a). Thus, negative $PC1_{OM}$-loadings likely
414 reflect a fresh pool of OM coming from in-lake vegetation.

415 $PC2_{OM}$ captures 14 % of the total variance and positive loadings are associated with (i) mid-
416 chain *n*-alkanes/*n*-alkenes doublets that are Py-products of resistant biomacromolecules such as
417 cutin, suberin and algaenan (Buurman and Roscoe, 2011); (ii) pristenes, resistant degradation
418 products of chlorophylls (Nguyen et al., 2003); and (iii) hopanoids, which are high-molecular
419 weight pentacyclic compounds of prokaryotes, especially bacteria, origin (Meredith et al., 2008;
420 Sessions et al., 2013). No compounds are significantly negatively correlated to $PC2_{OM}$ (Fig. 3a).
421 High $PC2_{OM}$ scores thus represent samples rich in organic molecules that are resistant to
422 degradation.

423 $PC3_{OM}$ explains 13 % of the total variance and separates carbohydrates and N-compounds that
424 are Py or degradation products of proteins, amino acids and/or chlorophylls (i.e., pyridines, ,
425 pyrroledione & pyrrolidinedione) and of chitin (positive loadings), from aliphatic long-chain *n*-

alkanes (C23-26:0 and C27-35:0) coming from cell wall lipids of higher plants or mosses (negative loadings; Fig. 3b).

On $PC4_{OM}$, which explains 13 % of the total variance, positive loadings are found for the diketopiperazines, i.e. specific Py products of proteins or amino acids, the alkylamides and the chlorophyll-derived phytadienes, ~~that~~ which altogether indicate fresh algal organic residues (Peulvé et al., 1996; Nguyen et al., 2003; Fabbri et al., 2005; Micić et al., 2010). Py products of chitin (Gupta et al., 2007), and hopanoids that are of prokaryotes, mainly bacteria, origin (Meredith et al., 2008; Sessions et al., 2013) also have positive loadings on $PC4_{OM}$, while no compounds are significantly negatively correlated to $PC4_{OM}$ (Fig. 3b). Therefore, $PC4_{OM}$ reflects OM input from in-lake algae and micro-organisms (e.g., zooplankton). Steroids, which have not yet been reported by Py-GC/MS in aquatic matrices, have positive loadings on this $PC4_{OM}$ suggesting that the steroids released by Py in aquatic samples are mainly of algal origin.

For $PC5_{OM}$, capturing 8 % of the total variance, positive loadings are related to lignin oligomers, which are specific for vascular plants (Meyers and Ishiwatari, 1993), and diketodipyrrole, a N-compound often reported in soil pyrolysates (e.g., Schellekens et al., 2009; Buurman and Roscoe, 2011). No compounds are associated with negative loadings on $PC5_{OM}$ (Fig. 3c). Interestingly, the long-chain *n*-alkanes from cell wall lipids of higher plants or mosses do not have positive loadings on $PC5_{OM}$. We therefore interpret $PC5_{OM}$ to relate to OM inputs from the forested catchment, which is dominated by coniferous species. Coniferous trees generally have higher lignin contents as compared to other vascular plants (Campbell and Sederof, 1996), while they contain much lower amounts of *n*-alkanes than other plant species (Bush and Mcinerney, 2013).

$PC6_{OM}$ captures 7 % of the total variance and has four compounds with significant positive loadings, i.e., benzene, two benzenes with oxidized side-chain and carboxy- or hydroxy-furans and furanones, i.e. furan and furanone heterocycles with an oxygen atom in the side-chain (Fig. 3c). $PC6_{OM}$ may represent an intermediate degradation status of higher plants and/or mosses residues,

between the lignin oligomers or ahnhydrosugars (fresh) and the degraded polyaromatics and benzenes C2-9 or (alkyl)furans and furanones (i.e. furan and furanone heterocycles with an aliphatic side-chain).

3.2.3 Cluster analysis of OM composition

As with the elemental geochemistry dataset, a solution of six clusters ($cluster_{OM}$ 1–6) was relevant to represent the data on the spatial heterogeneity of OM molecular composition (Fig. 1d). Each cluster is associated with one or a few of the OM types that were identified by the $PC1\text{-}6_{OM}$ (Fig. 3; Sect. 3.2.1). The cluster averages and standard deviations of each organic compound are given and compared to whole-lake averages in Table S5 in SI. Table 3 provides the cluster averages for ratios indicative of OM source types and their degradation status based on literature data and on the distribution of the organic compounds on $PC1\text{-}6_{OM}$.

In the south basin, the majority of sites found at shallower and intermediate water depths group in $cluster_{OM}$ 3 (n=14) and are enriched in degraded, resistant and bacterial OM (positive scores on $PC1_{OM}$; Fig. 3a). The deep basin sites ($cluster_{OM}$ 2; n=3) are enriched in fresh algal and zooplanktonic OM (positive scores on $PC4_{OM}$; Fig. 3b). Accordingly, the values for the ratios indicative of higher proportions of fresh, labile algal OM, based on N-compound or chlorophyll composition, are higher in the deeper sites as compared to whole-lake averages, while the values are below or within ±10 % of whole-lake averages in the sediments found at shallower and intermediate water depths (Table 1). In contrast, these two types of south basin sites have similar values, and lower as compared to whole-lake averages, for the ratios indicative of higher plant and moss OM freshness based on carbohydrate or lignin composition. Furthermore, the $clusters_{OM}$ 2 and 3 are characterized by higher values for the ratios specific of algal versus higher plant and moss OM based on the proportions of N-compounds versus carbohydrates or chlorophylls versus lignin

and long-chain *n*-alkanes and alkan-2-ones (Table 1). The rest of the south basin sites, fall within cluster$_{OM}$ 1 (n=1), 5 (n=2) or 4 (n=1), which are described below.

The majority of sites in the northern half of the lake group within cluster$_{OM}$ 1 (n=15) with isolated shallower sites falling within clusters$_{OM}$ 3 (n=1), 4 (n=2) and 5 (n=2). The sediments of cluster$_{OM}$ 1 are rich in fresh plant (higher plants or mosses) OM coming from in-lake productivity (negative scores on PC1$_{OM}$; Fig. 3a) and have higher values than whole-lake averages for the ratios specific of in-lake vs terrestrial plant OM and of higher plant and moss OM freshness (Table 1). In contrast, the values for these ratios are below 10% of whole-lake averages for the south basin sites, indicating that terrestrial input is the main source of plant OM to the sediments of the main basin of Härsvatten.

The cluster$_{OM}$ 5 represents some near-shore locations (n=4), which are enriched in OM derived from the coniferous-forested catchment (positive scores on PC5$_{OM}$; Fig. 3c). The cluster$_{OM}$ 4 (n=4), which groups shallow sites located close to the lake outlet (south basin, S16) and between the north and east basins (N10 and M1), is characterized by high proportions of degraded, resistant and bacterial OM (positive scores on PC5$_{OM}$; Fig. 3a). Two shallow sites of the central area (cluster$_{OM}$ 6; n=2) show an enrichment in aliphatic molecules derived from higher plant and moss cell wall lipids (negative loadings on PC3$_{OM}$; Fig. 3b). Both clusters$_{OM}$ 4 and 6 have values for the ratio indicative of in-lake:terrestrial plant OM above 10% of the whole-lake average, while the values for the ratios specific of algal vs higher plant and moss OM and of algal and plant OM freshness based on N-compounds and carbohydrates composition are below 10% of whole-lake averages (Table 1). Cluster$_{OM}$ 6 differs from cluster$_{OM}$ 4 by its higher values for the ratios specific of algal and higher plant OM freshness based on chlorophyll and lignin composition.

3.3 Factors and processes involved in the spatial distribution of OM molecular composition

The surface sediments used in this study comprise the uppermost 10 cm. Given the inherent variation in sedimentation rates across a lake basin, each bulk sample represents material deposited over different timescales. We know from the developmental work for our Py-GC/MS method using annually laminated sediments that there are transformations in OM composition within the uppermost few cm, i.e., the first few years following deposition (Tolu et al. 2015). Thus these bulk sediment samples provide initial insights into the spatial variability in molecular OM composition within a lake basin resulting from longer-term sedimentation processes (including those within the sediment) reflecting years to decades.

The distribution of both $clusters_{geo}$ and $clusters_{OM}$ within Härsvatten shows a similar general pattern (Fig. 1c and 1d) where a main feature is the separation of most of the sample locations from the north and east basins ($cluster_{geo}$ 1 and $cluster_{OM}$ 1) from those in the main south basin ($clusters_{geo}$ 2, 5, 6 and $clusters_{OM}$ 2, 3). The other similarities are i) the separation of the sediments within the main, south basin according to water depth, with $cluster_{geo}$ 5 and $cluster_{OM}$ 2 grouping the deeper sites and $clusters_{geo}$ 2, 6 and $cluster_{OM}$ 3 grouping the shallow and intermediate depth sites; and ii) the separation of the shallower sites that are located close to the shore ($cluster_{geo}$ 4 and $cluster_{OM}$ 5) from the ones that are found between the north and east basins and between the central area and the south basins ($cluster_{geo}$ 3 and $clusters_{OM}$ 4 and 6).

3.3.1 Spatial variability in the main south basin

As shown previously for OM (as % LOI) and Pb (Bindler et al. 2001), there is a physical and inorganic geochemical gradient from shallower to deeper waters reflecting sediment focusing in the south basin of Härsvatten. B.D. and bSi decrease from shallower ($cluster_{geo}$6) to intermediate ($cluster_{geo}$2) to deeper areas ($cluster_{geo}$5), whereas there is a progressive enrichment in organic

matter and trace elements with increasing water depth (Fig. 1c; Table 1). For example, B.D. decreases from ~0.07 to 0.03 g cm^{-3} while OM and Hg increase from ~34 to 52 % and from ~230 to 920 ng g^{-1}, respectively, in shallower versus the deepest locations. At intermediate depths ($cluster_{geo}2$), OM, B.D., bSi and most trace metals (i.e., Cu, Ni, Hg, Zn) are between those of shallow and deep locations. Sediment focusing is thus an important process for sediment geochemistry in the large, deep basin of Härsvatten, which presents a relatively simple morphometry. The sediments found at shallower (<11 m; $cluster_{geo}$ 6), intermediate (11-21 m; $cluster_{geo}$ 4) and deeper water depths (>23 m; $cluster_{geo}$ 5) would correspond approximatively to erosion, transportation and accumulation bottoms, respectively (Håkanson, 1977). The bSi decline, from ~15 to 4 %, indicates a decrease of diatom production with depth due to increasing light attenuation, and thus suggests that the diatom assemblage is dominated by benthic diatoms~~,~~ as shown for many acidified lakes, such as surrounding lakes in the Svartedalen nature reserve (e.g., Andersson, 1985; Anderson and Renberg, 1992).

In this main basin of Härsvatten, OM originates from a combination of autochthonous algal production and allochthonous input (Sect. 3.2.2). The dominance of benthic diatoms in acidified lakes and the declining bSi content with depth would indicate that the algal material in deeper areas of the basin should derive from resuspended benthic algal production. However, this benthic algal production is not reflected in the OM molecular composition. The sediments from shallow and intermediate water depths ($cluster_{OM}$ 3) are mainly composed of degraded, resistant and bacterial OM, while the sediments from deeper sites ($cluster_{OM}$ 2) are enriched in fresh algal OM (Fig. 1d; Sect. 3.2.2). Although our results are based on the top 10 cm of sediment and thus account for different sediment ages, we suggest that the higher proportions of decomposed algal material, based on N-compound and chlorophyll composition (Table 1), at shallower and intermediate water depths (<21m) than at the deepest sites (23.5–24.5 m) reflect higher mineralization rates of OM in shallow/intermediate areas. Higher OM mineralization rates in shallow/intermediate areas are most probably due to more oxic conditions, which are known to prevail in epilimnitic and metalimnitic

551 sediments (Ostovsky and Yacobi, 1999); the epilimnion in Härsvatten has been assessed to extend
552 to 10–15 m water depth. Higher OM preservation in the deeper area may also be favored by higher
553 accumulation rates as compared to shallow/intermediate areas (as consequence of sediment
554 focusing), but the sedimentation rates in the deeper areas of Härsvatten are nonetheless very low,
555 with the uppermost 30 cm being deposited during the last c. 500 year (Bindler et al., 2001).
556 Moreover, the elemental geochemistry indicates that the sites found at intermediate water depths
557 ($cluster_{geo}$ 6; 11–21 m) correspond in the sediment-focusing model to transportation zones, which
558 experience recurrent resuspension events that favor gas exchanges and mineralization of OM
559 (Ståhlberg et al., 2006). Occurrence of oxic conditions at intermediate depths in the south basin is
560 supported by the higher concentrations of Fe, Mn, As, Co and P and the high Fe:Al values, this
561 combination of parameters being often indicative of Fe and Mn (oxy)hydroxides (Table 1; Sect.
562 3.1.1). In line with our hypothesis, higher OM mineralization rates in oxic versus anoxic sediments
563 have previously been reported (Bastviken et al., 2004; Isidorova et al., 2016). However, in contrast
564 to the more algal-derived OM, we do not observe significant differences between the sediments of
565 shallower/intermediate water depth and the deepest sites for ratios indicative of higher plant and
566 moss OM freshness (Table 1). Because higher plant and moss OM is mainly of allochthonous
567 origin in this basin, our results indicate that primarily autochthonous algal OM is mineralized in the
568 epilimnitic and metalimnitic sediments of this deeper, steeper-sloped, basin of Härsvatten. This is
569 consistent with the suggestion that allochthonous OM is recalcitrant to sediment mineralization
570 after its degradation in the catchment and within the water column (Gudasz et al., 2012).

571 Overall, our molecular characterization of OM in the south basin suggests an enrichment in
572 algal versus allochthonous OM (e.g., higher N-compounds:carbohydrates) in the deeper areas of a
573 deep, simple lake basin, in line with previously reported sediment C:N ratios along lake-basin
574 transects (Kumke et al., 2005; Dunn et al., 2008; Bruesewitz et al., 2012). Given our data on the
575 degradation status of the different OM source-pools, we believe that this trend in OM quality results
576 from preferential degradation of algal versus allochthonous OM in sediments at

shallower/intermediate water depth in addition to the known focusing of living, and residues of, authochthonous OM towards deeper sites (Ostrovsky and Yacobi, 1999).

3.3.2 Spatial variability in the central, north and east basins and near-shore locations

In the northern half of the lake, 11 of 19 locations fall within $cluster_{geo}1$ (Fig. 1c), which distinguishes itself geochemically only by somewhat lower than average concentrations of elements often associated with (oxy)hydroxides (i.e., Fe, Mn, As, P and Co; Table 1 and Sect. 3.1.2). Sediments from the shallowest locations can potentially fall in one of four different clusters ($clusters_{geo}1$, 3, 4 or 6). Thus, for the northern half of the lake there is no evidence of sediment focusing. The effect is either limited by the more gentle slopes of the north and east basins (Blais and Kalff, 1995), modified by the water circulation resulting from the prevailing winds towards the north-east (Bindler et al. 2001, Abril et al., 2004), and/or interrupted by aquatic vegetation that acts as a sediment trap (Benoy and Kalff, 1999). Indeed, aquatic vegetation represents a major source of OM to the sediments of the northern, eastern and central basins ($clusters_{OM}$ 1, 4 and 6; Fig. 1d; Table 1 and Sect. 3.2.2). The enrichment of aquatic higher plant or moss OM in these sediments is consistent with field observations during the original sediment coring in winter 1997, where mosses and *Isoetes* (a vascular angiosperm plant) were observed in some parts of the lake to a depth of at least 10 m (Bindler et al., 2001). The presence of such submerged vegetation in Härsvatten is favored by its acidic, clear water (i.e., deeper light penetration), as previously observed for other acidified boreal Swedish lakes, such as the nearby lake Gårdsjön (Andersson, 1985; Grahn, 1985). Benthic aquatic vegetation is also favored in the northern half of Härsvatten by the more gentle slopes, comparatively shallow water depth and thus greater availability of light than in the deep, steeper-sloped south basin where allochthonous input appears as the main source of higher plant and moss OM (Sect. 3.2.2; Table 1).

602 The sediments found across the north and east basins and at the deeper sampling site of the
603 central area ($clusters_{OM}$ 1; Fig. 1d) have the highest proportions of fresh, labile higher plant and
604 moss OM (Sect. 3.2.2; Table 1). Also, the proportions of fresh, labile algal OM is as high as in the
605 deeper anoxic sediments of the main south basin and two times higher than in the sediments found
606 at shallow water depth in the south basin and central areas, although these sites span the same depth
607 range (3–11 m) and have relatively similar bSi contents (Table 1). These results indicate the
608 accumulation of fresh autochthonous, both plant and algal, OM in sediments associated with in-lake
609 vegetation even if they are below or within the epilimnion (i.e., supposed oxic conditions). A
610 possible explanation is that the input of labile, decomposing in-lake higher plant and moss OM
611 consumes oxygen and results in locally anoxic conditions in the sediment, which in turn lower OM
612 mineralization rates (Bastviken et al., 2004; Isidorova et al., 2016). This hypothesis may explain the
613 lower than whole-lake average concentrations of elements or elemental ratios often associated with
614 (oxy)hydroxides (i.e., Fe, Mn, As, Co, P contents and Fe:Al) in these epilimnitic/metaliminitic
615 sediments ($cluster_{geo}$ 1; Table 1). This interpretation is consistent with laboratory experiments,
616 where, for example, Kleeberg, 2013 had shown that inputs of macrophyte residues to sediments
617 results in oxygen depletion and microbially mediated reduction of Fe and Mn oxides. However, the
618 lower concentrations of Fe, Mn and other elements known to be associated with Fe and Mn
619 (oxy)hydroxides in these sediments of the north and south basins as compared to the sediments of
620 the south basin and to the whole-lake averages may also be related to shallow groundwater
621 discharges that are rich in (oxy)hydroxides or diagenetic processes that lead to Fe enrichment in the
622 sediments of the south basin.
623 The shallow sites located between the north and east basins and between the central area and
624 the south basin (i.e., $cluster_{geo}$ 3 and $clusters_{OM}$ 4 and 6; Fig. 1c and 1d) have higher than whole-lake
625 averages bSi contents and values for the ratio in-lake:terrestrial higher plant and moss OM,
626 suggesting that these sediments receive plant OM from in-lake vegetation and algal OM from
627 benthic production (Table 1). However, the proportions of fresh, labile plant and algal OM based on

628 N-compound and carbohydrate composition in these central sediments are much lower than in the
629 sediments found across the north and east basins (Table 1). Probably, these central areas are not
630 sites for aquatic vegetation growth, but receive in-lake plant OM produced within the north and east
631 basins that has been degraded during transport and/or is degraded at these shallow central sites due
632 to more oxic conditions as suggested by a higher occurrence of Fe and Mn (oxy)hydroxides (Fe,
633 Mn, As, Co, and P contents, Fe:Al and Mn:Fe above 10% of whole-lake averages; Table 1). Among
634 these shallow central sites, two locations ($cluster_{OM}$ 6) are specifically rich in higher plant and moss
635 lipids (i.e., C23-35:0; Table S3 in SI) and have high proportions of fresh higher plant OM based on
636 lignin composition (Table 1). This suggests preservation of higher plant cell-wall lipids and lignin
637 with respect to carbohydrates at these two shallow sites, in agreement with the known faster
638 assimilation of carbohydrates versus lipid and lignin structures (Bianchi and Canuel, 2011).
639 However, no reasonable hypothesis could be given to explain this difference in OM molecular
640 composition between the sediments at sites M5-6 and the ones at sites N10 and M1 given their
641 similar water depth and elemental geochemistry.
642 Among the sediments found in a small number of near-shore locations ($cluster_{geo}$ 4 and
643 $cluster_{OM}$ 5; n=4), three are located in two more-sheltered bays at the northwestern corner and the
644 southern end of the lake that are more protected from wind circulation (Bindler et al. 2001, Abril et
645 al. 2004). The sediments of these three locations predominantly accumulate terrestrial OM as
646 indicated by the abundance in lignin oligomers and the ratio indicative of in-lake:terrestrial plant
647 OM that are respectively above and below 10% of the whole-lake averages (Table 3).
648 Accumulation of OM coming from the coniferous-forested catchment most probably explained the
649 high OM content (i.e. 52-58% , which is as high as in the deeper sediments of the main south basin)
650 as well as the high concentrations of S and trace metals (i.e., Hg, Pb and Zn) in these near-shore
651 sediments (Table 1). Boreal forest soils are known to be enriched in S and trace metals because
652 their organic fraction retains atmospheric S and trace metals deposited over the industrial era
653 (Johansson and Tyler, 2001). Also, there is evidence that the transport of terrestrial OM to boreal

654 aquatic ecosystems is associated with significant inputs of trace metals (Grigal, 2002; Rydberg et
655 al., 2008). Alternatively, high S and trace metal contents could be due to accumulation of metal
656 sulfides due to near-shore groundwater gradients and/or anoxic conditions, or to redox cycling
657 related to the important input of terrestrial OM.
658
659 *3.3.3 Implication for in-lake and/or global elemental (e.g., C, nutrients, trace metals) cycling*
660
661 The molecular composition of natural OM has been shown to exert a strong influence on key
662 biogeochemical reactions involved in in-lake and global cycling of C, nutrients and trace metals,
663 such as C mineralization or nutrients/trace metals sorption and transformations into mobile and
664 bioavailable species (Drott A et al., 2007; Sobek et al., 2011; Gudasz et al., 2012; Tjerngren et al.,
665 2012; Kleeberg, 2013; Bravo et al., 2017). Our work demonstrates that OM molecular composition
666 can vary significantly within a single lake system in relation to basin morphometry, lake chemical
667 and biological status (e.g., presence of macrophytes, which is influenced by, e.g., acidification) and
668 the molecular structure/properties of the different OM compounds (e.g., higher resistant of
669 allochthonous versus autochthonous OM upon degradation). Our results further show that it may be
670 problematic to extrapolate data on OM composition from only a few sites or one basin when scaling
671 up to a whole lake. Thus, investigating sedimentary processes and the resulting fate of C and trace
672 elements using sampling strategies focused on the deepest area of a lake or on single transects from
673 shallower to deeper sites, may not fully capture the variation in either elemental geochemistry or
674 OM composition.
675 Overall, this study underlines that the OM molecular composition and its spatial heterogeneity
676 across a lake are two factors that should be considered to better constrain processes involved in the
677 fate of C, nutrients and trace metals in lake ecosystems, to improve whole-lake budgets for these
678 elements and to better assess pollution risks and the role of lakes in global elemental cycles.
679

Author contribution.

J. Tolu and R. Bindler designed research. J. Tolu performed Py-GC/MS analyses with help from L. Gerber and did the data treatment with the data processing pipeline of L. Gerber. J. Tolu and J. Rydberg performed XRF and mercury analyses. J. Tolu and C. Meyer-Jacob performed FTIR measurements and C. Meyer-Jacob determined the inferred bSi. J. Tolu, J. Rydberg, C. Meyer-Jacob and R. Bindler interpreted the data. J. Tolu prepared the manuscript with consistent contributions from J. Rydberg, R. Bindler and C. Meyer-Jacob.

Acknowledgements.

We would like to thank the university of Umeå (Sweden) for the funding of this work, which was supported by the environment's chemistry research group as well as the Umeå plant science center for making the Py-GC/MS available to us and Junko Takahashi Schmidt for the technical support in the Py-GC/MS laboratory.

References

Abril, J. M., El-Mrabet, R. and Barros, H.: The importance of recording physical and chemical variables simultaneously with remote radiological surveillance of aquatic systems: a perspective for environmental modelling, J. Environ. Radioactiv., 72, 145-152, 2004.

Amon, R. M. W. and Fitznar, H. P.: Linkages among the bioreactivity, chemical composition, and diagenetic state of marine dissolved organic matter, Limnol. Oceanogr., 46, 287-297, 2001.

Anderson, N. J. and Renberg, I.: A palaeolimnological assessment of diatom production responses to lake acidification, Environ. Pollut., 78, 113-119, 1992.

Andersson, B. I.: Properties and chemical composition of surficial sediments in the acidified Lake Gårdsjön, SW Sweden., Ecol. Bull., 37, 251–262, 1985.

Baas, M., Pancost, R., Van Geel, B. and Sinninghe Damsté, J. S.: A comparative study of lipids in Sphagnum species, Org. Geochem., 31, 535-541, 2000.

706 Ball, D. F.: Loss-on-ignition as estimate of organic matter and organic carbon in non-
707 calcareous soils, J. Soil Sci., 15, 84-92, 1964.
708 Bastviken, D., Persson, L., Odham, G. and Tranvik, L.: Degradation of dissolved organic
709 matter in oxic and anoxic lake water, Limnol. Oceanogr., 49, 109-116, 2004.
710 Benoy, G. A. and Kalff, J.: Sediment accumulation and Pb burdens in submerged macrophyte
711 beds, Limnol. Oceanogr., 44, 1081-1090, 1999.
712 Bianchi, T. S. and Canuel, E. A.: Chapter 2: Chemical biomarkers application to ecology and
713 paleoecology, in: Chemical biomarkers in aquatic ecosystems, Princeton University press,
714 Princeton (New Jersey, USA), 19-29, 2011.
715 Bindler, R., Renberg, I., Brannvall, M. L., Emteryd, O. and El-Daoushy, F.: A whole-basin
716 study of sediment accumulation using stable lead isotopes and flyash particles in an acidified lake,
717 Sweden, Limnol. Oceanogr., 46, 178-188, 2001.
718 Blais, J. M. and Kalff, J.: The influence of lake morphometry on sediment focusing, Limnol.
719 Oceanogr., 40, 582-588, 1995.
720 Bravo, A. G., Bouchet, S., Tolu, J., Björn, E., Mateos-Rivera, A. and Bertilsson, S.:
721 Molecular composition of organic matter controls methylmercury formation in boreal lakes, Nature
722 Communications, 8, 14255, 2017.
723 Bruesewitz, D. A., Tank, J. L. and Hamilton, S. K.: Incorporating spatial variation of
724 nitrification and denitrification rates into whole-lake nitrogen dynamics, J. Geophys. Res.-Biogeo.,
725 117, 2012.
726 Bush, R. T. and Mcinerney, F. A.: Leaf wax n-alkane distributions in and across modern
727 plants: Implications for paleoecology and chemotaxonomy, Geochim. Cosmochim. Ac., 117, 161-
728 179, 2013.
729 Buurman, P., Van Bergen, P. F., Jongmans, A. G., Meijer, E. L., Duran, B. and Van Lagen,
730 B.: Spatial and temporal variation in podzol organic matter studied by pyrolysis-gas
731 chromatography/mass spectrometry and micromorphology, Eur. J. Soil Sci., 56, 253-270, 2005.

Buurman, P. and Roscoe, R.: Different chemical composition of free light, occluded light and extractable SOM fractions in soils of Cerrado and tilled and untilled fields, Minas Gerais, Brazil: A pyrolysis-GC/MS study, Eur. J. Soil Sci., 62, 253-266, 2011.

Campbell, M. M. and Sederof, R. R.: Variation in Lignin Content and Composition, Plant Physiol., 110, 3-13, 1996.

Carr, A. S., Boom, A., Chase, B. M., Roberts, D. L. and Roberts, Z. E.: Molecular fingerprinting of wetland organic matter using pyrolysis-GC/MS: An example from the southern Cape coastline of South Africa, J. Paleolimnol., 44, 947-961, 2010.

Dauwe, B. and Middelburg, J. J.: Amino acids and hexosamines as indicators of organic matter degradation state in North Sea sediments, Limnol. Oceanogr., 43, 782-798, 1998.

De La Rosa, J. M., González-Pérez, J. A., González-Vila, F. J., Knicker, H. and Araújo, M. F.: Molecular composition of sedimentary humic acids from South West Iberian Peninsula: A multi-proxy approach, Org. Geochem., 42, 791-802, 2011.

Drott A, Lambertsson L, Bjorn E and U, S.: Importance of dissolved neutral mercury sulfides for methyl mercury production in contaminated sediments, Environ. Sci. Technol., 41, 2270-2276, 2007.

Dunn, R. J. K., Welsh, D. T., Teasdale, P. R., Lee, S. Y., Lemckert, C. J. and Meziane, T.: Investigating the distribution and sources of organic matter in surface sediment of Coombabah Lake (Australia) using elemental, isotopic and fatty acid biomarkers, Cont. Shelf Res., 28, 2535-2549, 2008.

Fabbri, D., Sangiorgi, F. and Vassura, I.: Pyrolysis-GC-MS to trace terrigenous organic matter in marine sediments: A comparison between pyrolytic and lipid markers in the Adriatic Sea, Anal. Chim. Acta, 530, 253-261, 2005.

Faix, O., Meier, D. and Fortmann, I.: Thermal degradation products of wood: gas chromatographic separation and mass spectrometric characterization of monomeric lignin derived products, Holz als Roh- und Werkstoff, 48, 281-285, 1990.

Faix, O., Fortmann, I., Bremer, J. and Meier, D.: Thermal degradation products of wood: gas chromatographic separation and mass spectrometric characterization of polysaccharide derived products, Holz als Roh- und Werkstoff, 49, 213-219, 1991.

Fichez, R.: Composition and fate of organic matter in submarine cave sediments; implications for the biogeochemical cycle of organic carbon, Oceanologica Acta, 14, 369-377, 1991.

Grahn, O.: Macrophyte biomass and production in Lake Gårdsjön - an acidified clearwater lake in the SW Sweden., Ecol. Bull., 37, 203–212, 1985.

Grigal, D. F.: Inputs and outputs of mercury from terrestrial watersheds: a review, Environ. Rev., 10, 1-39, 2002.

Gudasz, C., Bastviken, D., Premke, K., Steger, K. and Tranvik, L. J.: Constrained microbial processing of allochthonous organic carbon in boreal lake sediments, Limnol. Oceanogr., 57, 163-175, 2012.

Gupta, N. S., Briggs, D. E. G., Collinson, M. E., Evershed, R. P., Michels, R. and Pancost, R. D.: Molecular preservation of plant and insect cuticles from the Oligocene Enspel Formation, Germany: Evidence against derivation of aliphatic polymer from sediment, Org. Geochem., 38, 404-418, 2007.

Håkanson, L.: The influence of wind, fetch and water depth on the distribution of sediments in Lake Vanern, Sweden., Can. J. Earth Sci., 14, 397-412, 1977.

Hawkes, J. A., Dittmar, T., Patriarca, C., Tranvik, L. and Bergquist, J.: Evaluation of the Orbitrap Mass Spectrometer for the Molecular Fingerprinting Analysis of Natural Dissolved Organic Matter, Analytical Chemistry, 88, 7698-7704, 2016.

Heathcote, A. J., Anderson, N. J., Prairie, Y. T., Engstrom, D. R. and Del Giorgio, P. A.: Large increases in carbon burial in northern lakes during the Anthropocene, Nature Communications, 6, 2015.

Hernandez, M. E., Mead, R., Peralba, M. C. and Jaffé, R.: Origin and transport of n-alkane-2-ones in a subtropical estuary: Potential biomarkers for seagrass-derived organic matter, Org. Geochem., 32, 21-32, 2001.

Isidorova, A., Bravo, A. G., Riise, G., Bouchet, S., Bjorn, E. and Sobek, S.: The effect of lake browning and respiration mode on the burial and fate of carbon and mercury in the sediment of two boreal lakes, J. Geophys. Res.-Biogeo., 121, 233-245, 2016.

Johansson, K. and Tyler, G.: Impact of atmospheric long range transport of lead, mercury and cadmium on the Swedish forest environment, Water, Air Soil Pollut., 425, 279-297, 2001.

Jokic, A., Schulten, H. R., Cutler, J. N., Schnitzer, M. and Huang, P. M.: A significant abiotic pathway for the formation of unknown nitrogen in nature, Geophys. Res. Lett., 31, L05502 1-4, 2004.

Kaal, J., Baldock, J. A., Buurman, P., Nierop, K. G. J., Pontevedra-Pombal, X. and Martínez-Cortizas, A.: Evaluating pyrolysis-GC/MS and 13C CPMAS NMR in conjunction with a molecular mixing model of the Penido Vello peat deposit, NW Spain, Org. Geochem., 38, 1097-1111, 2007.

Kellerman, A. M., Dittmar, T., Kothawala, D. N. and Tranvik, L. J.: Chemodiversity of dissolved organic matter in lakes driven by climate and hydrology, Nature Communications, 4804, 2014.

Kellerman, A. M., Kothawala, D. N., Dittmar, T. and Tranvik, L. J.: Persistence of dissolved organic matter in lakes related to its molecular characteristics, Nature Geoscience, 8, 454-457, 2015.

Kleeberg, A.: Impact of aquatic macrophyte decomposition on sedimentary nutrient and metal mobilization in the initial stages of ecosystem development, Aquat. Bot., 105, 41-49, 2013.

Koinig, K. A., Shotyk, W., Lotter, A. F., Ohlendorf, C. and Sturm, M.: 9000 years of geochemical evolution of lithogenic major and trace elements in the sediment of an alpine lake - the role of climate, vegetation, and land-use history, J. Paleolimnol., 30, 307-320, 2003.

807 Korsman, T., Nilsson, M. B., Landgren, K. and Renberg, I.: Spatial variability in surface
808 sediment composition characterised by near-infrared (NIR) reflectance spectroscopy, J.
809 Paleolimnol., 21, 61-71, 1999.
810 Kumke, T., Schoonderwaldt, A. and Kienel, U.: Spatial variability of sedimentological
811 properties in a large Siberian lake, Aquat. Sci., 67, 86-96, 2005.
812 Lehtonen, T., Peuravuori, J. and Pihlaja, K.: Degradation of TMAH treated aquatic humic
813 matter at different temperatures, J. Anal. Appl. Pyrol., 55, 151-160, 2000.
814 Leri, A. C. and Myneni, S. C. B.: Natural organobromine in terrestrial ecosystems, Geochim.
815 Cosmochim. Ac., 77, 1-10, 2012.
816 Lidman, F., Kohler, S. J., Morth, C. M. and Laudon, H.: Metal Transport in the Boreal
817 Landscape-The Role of Wetlands and the Affinity for Organic Matter, Environ. Sci. Technol., 48,
818 3783-3790, 2014.
819 Marbot, R.: The selection of pyrolysis temperatures for the analysis of humic substances and
820 related materials .1. Cellulose and chitin, J. Anal. Appl. Pyrol., 39, 97-104, 1997.
821 Mcclymont, E. L., Bingham, E. M., Nott, C. J., Chambers, F. M., Pancost, R. D. and
822 Evershed, R. P.: Pyrolysis GC-MS as a rapid screening tool for determination of peat-forming plant
823 composition in cores from ombrotrophic peat, Org. Geochem., 42, 1420-1435, 2011.
824 Meredith, W., Snape, C. E., Carr, A. D., Nytoft, H. P. and Love, G. D.: The occurrence of
825 unusual hopenes in hydropyrolysates generated from severely biodegraded oil seep asphaltenes,
826 Org. Geochem., 39, 1243-1248, 2008.
827 Meyer-Jacob, C., Vogel, H., Boxberg, F., Rosen, P., Weber, M. E. and Bindler, R.:
828 Independent measurement of biogenic silica in sediments by FTIR spectroscopy and PLS
829 regression, J. Paleolimnol., 52, 245-255, 2014.
830 Meyers, P. A. and Ishiwatari, R.: Lacustrine organic geochemistry-an overview of indicators
831 of organic matter sources and diagenesis in lake sediments, Org. Geochem., 20, 867-900, 1993.

Micić, V., Kruge, M., Körner, P., Bujalski, N. and Hofmann, T.: Organic geochemistry of Danube River sediments from Pančevo (Serbia) to the Iron Gate dam (Serbia-Romania), Org. Geochem., 41, 971-974, 2010.

Micić, V., Kruge, M. A., Köster, J. and Hofmann, T.: Natural, anthropogenic and fossil organic matter in river sediments and suspended particulate matter: A multi-molecular marker approach, Sci. Total Environ., 409, 905-919, 2011.

Mucci, A., Richard, L. F., Lucotte, M. and Guignard, C.: The differential geochemical behavior of arsenic and phosphorus in the water column and sediments of the Saguenay Fjord estuary, Canada, Aquat. Geochem., 6, 293-324, 2000.

Naeher, S., Gilli, A., North, R. P., Hamann, Y. and Schubert, C. J.: Tracing bottom water oxygenation with sedimentary Mn/Fe ratios in Lake Zurich, Switzerland, Chem. Geol., 352, 125-133, 2013.

Nguyen, R. T., Harvey, H. R., Zang, X., Van Heemst, J. D. H., Hetényi, M. and Hatcher, P. G.: Preservation of algaenan and proteinaceous material during the oxic decay of Botryococcus braunii as revealed by pyrolysis-gas chromatography/mass spectrometry and 13C NMR spectroscopy, Org. Geochem., 34, 483-497, 2003.

Nichols, J. E. and Huang, Y.: C23-C31 n-alkan-2-ones are biomarkers for the genus Sphagnum in freshwater peatlands, Org. Geochem., 38, 1972-1976, 2007.

Nierop, K. G. J. and Buurman, P.: Composition of soil organic matter and its water-soluble fraction under young vegetation on drift sand, central Netherlands, Eur. J. Soil Sci., 49, 605-615, 1998.

Ostrovsky, I. and Yacobi, Y. Z.: Organic matter and pigments in surface sediments: possible mechanisms of their horizontal distributions in a stratified lake, Can. J. Fish. Aquat. Sci., 56, 1001-1010, 1999.

Page, D. W.: Characterisation of organic matter in sediment from Corin Reservoir, Australia, J. Anal. Appl. Pyrol., 70, 169-183, 2003.

858 Peulvé, S., Sicre, M. A., Saliot, A., De Leeuw, J. W. and Baas, M.: Molecular
859 characterization of suspended and sedimentary organic matter in an Arctic delta, Limnol.
860 Oceanogr., 41, 488-497, 1996.
861 Plant, J. A., Kinniburgh, D. G., Smedley, P. L., Fordyce, F. M. and Klinck, B. A.: Arsenic and
862 selenium, in: Environmental geochemistry : treatise on geochemistry Volume 9, B. S. Lollar,
863 Elsevier, Amsterdam, The Netherlands, 17-66, 2005.
864 Rydberg, J., Gälman, V., Ingemar, R., Bindler, R., Lambertsson, L. and Martinez-Cortizas,
865 A.: Assessing the Stability of Mercury and Methylmercury in a Varved Lake Sediment Deposit,
866 Environ. Sci. Technol., 42, 4391-4396, 2008.
867 Rydberg, J., Rosen, P., Lambertsson, L., De Vleeschouwer, F., Tomasdotter, S. and Bindler,
868 R.: Assessment of the spatial distributions of total- and methyl-mercury and their relationship to
869 sediment geochemistry from a whole-lake perspective, J. Geophys. Res.-Biogeo., 117, 2012.
870 Rydberg, J.: Wavelength dispersive X-ray fluorescence spectroscopy as a fast, non-
871 destructive and cost-effective analytical method for determining the geochemical composition of
872 small loose-powder sediment samples, J. Paleolimnol., 52, 265-276, 2014.
873 Santisteban, J. I., Mediavilla, R., Lopez-Pamo, E., Dabrio, C. J., Zapata, M. B. R., Garcia, M.
874 J. G., Castano, S. and Martinez-Alfaro, P. E.: Loss on ignition: a qualitative or quantitative method
875 for organic matter and carbonate mineral content in sediments?, J. Paleolimnol., 32, 287-299, 2004.
876 Sarkar, S., Wilkes, H., Prasad, S., Brauer, A., Riedel, N., Stebich, M., Basavaiah, N. and
877 Sachse, D.: Spatial heterogeneity in lipid biomarker distributions in the catchment and sediments of
878 a crater lake in central India, Org. Geochem., 66, 125-136, 2014.
879 Schellekens, J., Buurman, P. and Pontevedra-Pombal, X.: Selecting parameters for the
880 environmental interpretation of peat molecular chemistry - A pyrolysis-GC/MS study, Org.
881 Geochem., 40, 678-691, 2009.
882

Schulten, H. R. and Gleixner, G.: Analytical pyrolysis of humic substances and dissolved organic matter in aquatic systems: Structure and origin, Water Res., 33, 2489-2498, 1999.

Sessions, A. L., Zhang, L., Welander, P. V., Doughty, D., Summons, R. E. and Newman, D. K.: Identification and quantification of polyfunctionalized hopanoids by high temperature gas chromatography-mass spectrometry, Org. Geochem., 56, 120-130, 2013.

Sinninghe Damsté, J. S., Eglinton, T. I. and De Leeuw, J. W.: Alkylpyrroles in a kerogen pyrolysate: Evidence for abundant tetrapyrrole pigments, Geochim. Cosmochim. Ac., 56, 1743-1751, 1992.

Sobek, S., Algesten, G., Bergstrom, A. K., Jansson, M. and Tranvik, L. J.: The catchment and climate regulation of pCO(2) in boreal lakes, Glob. Change Biol., 9, 630-641, 2003.

Sobek, S., Zurbrugg, R. and Ostrovsky, I.: The burial efficiency of organic carbon in the sediments of Lake Kinneret, Aquat. Sci., 73, 355-364, 2011.

Ståhlberg, C., Bastviken, D., Svensson, B. H. and Rahm, L.: Mineralisation of organic matter in coastal sediments at different frequency and duration of resuspension, Estuar. Coast. Shelf S., 70, 317-325, 2006.

Stewart, C. E.: Evaluation of angiosperm and fern contributions to soil organic matter using two methods of pyrolysis-gas chromatography-mass spectrometry, Plant and Soil, 351, 31-46, 2012.

Stubbins, A. and Dittmar, T.: Illuminating the deep: Molecular signatures of photochemical alteration of dissolved organic matter from North Atlantic Deep Water, Marine Chemistry, 177, 318-324, 2015.

Taboada, T., Cortizas, A. M., Garcia, C. and Garcia-Rodeja, E.: Particle-size fractionation of titanium and zirconium during weathering and pedogenesis of granitic rocks in NW Spain, Geoderma, 131, 218-236, 2006.

907 Tesi, T., Langone, L., Goñi, M. A., Wheatcroft, R. A., Miserocchi, S. and Bertotti, L.: Early
908 diagenesis of recently deposited organic matter: A 9-yr time-series study of a flood deposit,
909 Geochim. Cosmochim. Ac., 83, 19-36, 2012.
910 Tjerngren, I., Meili, M., Bjorn, E. and Skyllberg, U.: Eight Boreal Wetlands as Sources and
911 Sinks for Methyl Mercury in Relation to Soil Acidity, C/N Ratio, and Small-Scale Flooding,
912 Environ. Sci. Technol., 46, 8052-8060, 2012.
913 Tranvik, L. J., Downing, J. A., Cotner, J. B., Loiselle, S. A., Striegl, R. G., Ballatore, T. J.,
914 Dillon, P., Finlay, K., Fortino, K., Knoll, L. B., Kortelainen, P. L., Kutser, T., Larsen, S., Laurion,
915 I., Leech, D. M., Leigh Mccallister, S., Mcknight, D. M., Melack, J. M., Overholt, E., Porter, J. A.,
916 Prairie, Y., Renwick, W. H., Roland, F., Sherman, B. S., Schindler, D. W., Sobek, S., Tremblay, A.,
917 Vanni, M. J., Verschoor, A. M., Von Wachenfeldt, E. and Weyhenmeyer, G. A.: Lakes and
918 reservoirs as regulators of carbon cycling and climate, Limnol. Oceanogr., 54, 2298-2314, 2009.
919 Trolle, D., Zhu, G. W., Hamilton, D., Luo, L. C., Mcbride, C. and Zhang, L.: The influence of
920 water quality and sediment geochemistry on the horizontal and vertical distribution of phosphorus
921 and nitrogen in sediments of a large, shallow lake, Hydrobiologia, 627, 31-44, 2009.
922 Valdes, F., Catala, L., Hernandez, M. R., Garcia-Quesada, J. C. and Marcilla, A.:
923 Thermogravimetry and Py-GC/MS techniques as fast qualitative methods for comparing the
924 biochemical composition of Nannochloropsis oculata samples obtained under different culture
925 conditions, Bioresource Technol., 131, 86-93, 2013.
926 Vancampenhout, K., Wouters, K., Caus, A., Buurman, P., Swennen, R. and Deckers, J.:
927 Fingerprinting of soil organic matter as a proxy for assessing climate and vegetation changes in last
928 interglacial palaeosols (Veldwezelt, Belgium), Quaternary Research, 69, 145-162, 2008.
929 Vogel, H., Wessels, M., Albrecht, C., Stich, H. B. and Wagner, B.: Spatial variability of
930 recent sedimentation in Lake Ohrid (Albania/Macedonia), Biogeosciences, 7, 3333-3342, 2010.

Wagner, S., Jaffé, R., Cawley, K., Dittmar, T. and Stubbins, A.: Associations between the molecular and optical properties of dissolved organic matter in the Florida Everglades, a model coastal wetland system, Frontiers in Chemistry, 3, 2015.

Wakeham, S. G., Lee, C., Hedges, J. I., Hernes, P. J. and Peterson, M. L.: Molecular indicators of diagenetic status in marine organic matter, Geochim. Cosmochim. Ac., 61, 5363-5369, 1997.

Yin, H., Feng, X. H., Qiu, G. H., Tan, W. F. and Liu, F.: Characterization of Co-doped birnessites and application for removal of lead and arsenite, J. Hazard. Mater., 188, 341-349, 2011.

Zheng, Y. H., Zhou, W. J. and Meyers, P. A.: Proxy value of n-alkan-2-ones in the Hongyuan peat sequence to reconstruct Holocene climate changes on the eastern margin of the Tibetan Plateau, Chem. Geol., 288, 97-104, 2011.

Zhu, M. Y., Zhu, G. W., Li, W., Zhang, Y. L., Zhao, L. L. and Gu, Z.: Estimation of the algal-available phosphorus pool in sediments of a large, shallow eutrophic lake (Taihu, China) using profiled SMT fractional analysis, Environ. Pollut., 173, 216-223, 2013.

Tables

Table 1. Summary statistics for sediment elemental geochemistry

		Whole sample collection except the two outliers					Outliers (M4, S15)			
	Unit	**Av.**[a] ± sd[b]	**CV**[c]	**Median**	**A:M**[d]	**Min**[e]**-Max**[f]	**Av. ± sd**	**CV**[c]	**Median**	**Min-Max**
W.D.	m	**9** ± 7	*74*	7	*1.23*	2-25	**3.4** ± 0.6	*19*	3	2.9-3.8
B.D.	g cm^{-3}	**0.06** ± 0.02	*38*	0.06	*1.05*	0.02-0.13	**0.67** ± 0.09	*14*	0.06	0.61-0.74
bSi	%	**13** ± 6	*48*	12	*1.05*	4-25	**1.9** ± 0.2	*0*	12	1.7-2.0
LOI	%	**38** ± 10	*26*	37	*1.01*	10-58	**3.6** ± 0.8	*20*	37	3.0-4.1
[S]	mg kg^{-1}	**11876** ± 5920	*50*	11305	*1.05*	4685-29190	**2570** ± 552	*21*	10610	2180-2960
[Br]	mg kg^{-1}	**149** ± 35	*23*	152	*0.99*	71-225	**16** ± 7	*44*	148	11-21
[Cu]	mg kg^{-1}	**34** ± 13	*37*	32	*1.07*	12-75	**9** ± 3	*31*	31	7-11
[Ni]	mg kg^{-1}	**19** ± 4	*24*	19	*0.99*	10-27	**12** ± 4	*35*	19	9-15
[Hg]	µg kg^{-1}	**337** ± 202	*60*	286	*1.18*	117-1152	**28** ± 9	*33*	274	21-34
[Pb]	mg kg^{-1}	**192** ± 74	*39*	184	*1.05*	58-422	**22** ± 16	*76*	178	10-33
[Zn]	mg kg^{-1}	**219** ± 108	*49*	207	*1.06*	43-445	**50** ± 16	*31*	200	39-61
[Al]	%	**3** ± 1	*17*	3	*1.06*	2-4	**5.67** ± 0.01	*0.1*	3	5.66-5.67
[Y]	mg kg^{-1}	**25** ± 8	*32*	25	*1.01*	7-43	**20** ± 4	*18*	25	17-22
[Fe]	%	**5** ± 3	*65*	4	*1.26*	1-12	**3.4** ± 0.1	*4*	4	3.3-3.5
[As]	mg kg^{-1}	**35** ± 20	*56*	28	*1.26*	5-73	<DL		27	0-0
[P]	mg kg^{-1}	**1624** ± 741	*46*	1401	*1.16*	655-3769	**949** ± 57	*6*	1389	908-989
[Mn]	mg kg^{-1}	**729** ± 1690	*232*	180	*4.06*	94-7981	**1060** ± 845	*80*	184	462-1657
[Co]	mg kg^{-1}	**19** ± 15	*77*	14	*1.39*	5-76	**17** ± 9	*56*	14	10-23
[Ca]	mg kg^{-1}	**5261** ± 1306	*25*	5213	*1.01*	2860-9300	**26540** ± 7566	*29*	5283	21190-31890
[K]	mg kg^{-1}	**4426** ± 1020	*23*	4485	*0.99*	2420-6140	**10510** ± 2616	*25*	4580	8660-12360
[Mg]	mg kg^{-1}	**1488** ± 354	*24*	1500	*0.99*	870-2130	**7495** ± 3599	*48*	1515	4950-10040
[Na]	mg kg^{-1}	**1795** ± 659	*37*	1743	*1.03*	440-3380	**10695** ± 587	*5*	1783	10280-11110
[$Si_{inorganic}$]	%	**11** ± 4	*33*	11	*1.06*	4-21	**23** ± 1	*3*	11	22-23
[Sr]	mg kg^{-1}	**55** ± 16	*29*	55	*1.01*	27-116	**235** ± 24	*10*	55	218-252
[Ti]	mg kg^{-1}	**2115** ± 495	*23*	2200	*0.96*	997-2870	**4357** ± 2348	*54*	2215	2697-6017
[V]	mg kg^{-1}	**63** ± 15	*23*	60	*1.05*	36-101	**75** ± 23	*31*	60	58-91
[Zr]	mg kg^{-1}	**101** ± 31	*31*	100	*1.01*	39-160	**158** ± 6	*4*	103	153-162

[a] Av.: average; [b]sd: standard deviation; [c]CV: coefficient of variation calculated as relative standard deviation in %; [d]A:M: ratio between average and median Min.: minimal values; [e]Max.: maximal value

Table 2. Summary statistics for the molecular composition of sediment OM given as relative abundances (expressed in %) of the 41 groups of Py organic compounds, which belong to 13 classes of OM that are indicated by the grey shading *(to be continued)*

	Compounds included	**Av[a]** ± sd	**CV**	**Median**	**A:M**	**Min-Max**
Carbohydrates						
(Alkyl)-furans &furanones	3-furaldehyde, 2-furaldehyde, 2-acetyl-furan, Methyl-3-furaldehyde, 2(5H)-furanone, Methyl-2-furaldehyde, Dihydro-methyl-furanone, Methyl-2(5H)-furanone, Methyl-2-furaldehyde	**15** ± 4	30	*14*	1.06	8-28
Hydroxy- or carboxy-furans & furanones	2-Furancarboxylic acid, methyl ester; 2,5-Dimethyl-4-hydroxy-3(2H)-furanone; 5-(hydroxymethyl)-2-furaldehyde	**4.1** ± 1.2	29	*4.0*	1.03	0.8-7.5
Pyrans	5,6-dihydro-pyran-2-one, 4-hydroxy-5,6-dihydro-pyran-2-one	**3.4** ± 1	30	*3.2*	1.06	1.2-5.3
Dianhydrorhamnose	Dianhydrorhamnose	**1.6** ± 0.5	28	*1.7*	0.99	0.3-2.7
Levoglucosenone	Levoglucosenone	**2.2** ± 0.4	20	*2.2*	1.00	1.3-3.1
Anhydrosugars	Anhydrohexose, Levogalactosan, Levomannosan, Levoglucosan	**3.7** ± 2.6	71	*2.5*	1.46	0.8-11
Chitin derived compounds						
Chitin-derived compounds	Acetamide, 3-acetamido-furan, 3-acetamido-4-pyrone, Oxazoline	**2.5** ± 1	40	*2.6*	0.98	0.2-4.2
N-compounds						
(Alkyl)pyridines	Pyridine, 2-methyl-pyridine, 3/4-methyl-pyridine	**0.3** ± 0.1	34	*0.3*	0.95	0.1-0.5
Pyridines_O, i.e. pyridines with side chain containing a ”C=O” function	2-acetylpyridine, 3-acetylpyridine, 2-Methyl-5-acetoxypyridine	**0.7** ± 0.1	18	*0.7*	1.00	0.2-0.9
(Alkyl)pyrroles	Pyrrole, Methyl-pyrrole	**2.4** ± 0.5	22	*2.4*	1.01	1.7-3.5
Pyrroles_O , i.e. pyrroles with side chain containing a ”C=O” function	2-formyl-pyrrole, 2-acetyl-pyrrole, 2-formyl-1-methylpyrrole	**1.0** ± 0.2	25	*0.9*	1.04	0.5-1.4
Pyrroledione & pyrrolidinedione	2,5-pyrroledione, 2,5-pyrrolidinedione	**1.2** ± 0.3	29	*1.2*	0.98	0.2-1.7
Aromatic N- compounds	Benzeneacetonitrile, Benzenepropanenitrile	**0.8** ± 0.3	36	*0.8*	1.03	0.3-1.4
Indoles	Indole, Methyl-indole	**1.5** ± 0.4	24	*1.5*	1.03	0.5-3.1
Diketodipyrrole	Diketodipyrrole	**0.8** ± 0.2	22	*0.8*	1.01	0.4-1.2
Diketopiperazines	Pro-Ala, Pro-Val, Pro-Val, Cyclo-Leu-Pro, Pro-Pro, Pro-Phe	**1.5** ± 0.4	30	*1.5*	1.02	0.3-2.6
Alkylamides	6 alkylamides	**0.6** ± 0.3	51	*0.6*	1.06	0.1-1.7
Phenols						
Phenols	Phenol, 2-methyl-phenol, 3/4- methyl-phenol, dimethyl-phenol, Ethyl-phenol, Propenyl-phenol	**8** ± 1	15	*8*	1.02	4.4-11.4
Lignins						
Syringols	Syringol, 4-vinyl-syringol, 4-formyl-syringol, 4-allenesyringol, Acetosyringone	**0.5** ± 0.4	83	*0.4*	1.32	0.1-1.9
Guaiacols	Guaiacol, Ethyl-guaiacol, 4-vinyl-guaiacol, 4-propenyl-guaiacol, Vanillin, 4-alleneguaiacol, Acetovanillone, Vanillic acid, methyl ester, Guaiacylacetone	**3.6** ± 2.3	65	*2.9*	1.24	1.1-13.5

Table 2. Summary statistics for the molecular composition of sediment OM given as the relative abundances (expressed in %) of the 41 groups of Py organic compounds, which belong to 13 classes of OM that are indicated by the grey shading *(following part)*

Chlorophylls						
Pristenes	Prist-1-ene, Prist-2-ene	**2.7** ± 0.8	28	*2.8*	0.97	0.4-4.6
Phytadienes	Phytadiene 1, Phytadiene 2	**1.9** ± 0.7	35	*1.8*	1.04	0.2-3.6
***n*-alkenes**						
C9-16:1	*n*-alkenes C9, C13, C14, C16	**3.5** ± 0.8	23	*3.6*	0.98	1.8-5.1
C17-C22:1	*n*-alkenes C17, C18, C19, C20, C21, C22	**6** ± 1	17	*6.2*	0.97	3.5-8.9
C23-26_1	*n*-alkenes C23, C24, C25, C26	**2.9** ± 0.9	32	*2.7*	1.09	0.6-5.4
C27-28:1	*n*-alkenes C27, C28	**0.8** ± 0.4	47	*0.7*	1.10	0.1-1.4
***n*-alkanes**						
C10-16:0	*n*-alkanes C10, C11, C12, C13, C14, C15, C16	**2.5** ± 0.6	23	*2.5*	1.03	1.3-4.1
C17-22:0	*n*-alkanes C17, C18, C19, C20, C21, C22	**3.9** ± 0.8	21	*4.0*	0.98	1.6-5.4
C23-26:0	*n*-alkanes C23, C24, C25, C26	**2.8** ± 1.4	49	*2.7*	1.07	1.4-8.8
C27-35:0	*n*-alkanes C27, C28, C29, C30, C31, C32, C33, C35	**4.3** ± 3.5	80	*3.6*	1.20	1.1-21.3
Alkan-2-ones						
2K C13-17	Alkan-2-ones C13, 16, 17	**1.3** ± 0.4	33	*1.4*	0.96	0.6-2.2
2K C19-21	Alkan-2-ones C19, 20, 21	**0.3** ± 0.1	45	*0.3*	0.97	0-0.8
2K C23-31	Alkan-2-ones C23, 14, 25, 26, 27, 28, 29, 31	**1.3** ± 0.8	62	*1.1*	1.24	0.1-3.3
Steroids						
Steroids	Cholest-2-ene, Cholesta-3,5-diene, Stigmasta-5,22-dien-3-ol, acetate, Sitosterol, Cholesta-3,5-dien-7-one, Stigmasta-3,5-dien-7-one	**1.2** ± 0.9	70	*1.1*	1.10	0-4.3
Tocopherols						
Tocopherols	γ-Tocopherol, α-Tocopherol	**0.3** ± 0.3	106	*0.2*	1.75	0-1.5
Hopanoids						
Hopanoids	Trinosphopane, Norhopene, 22,29,30-trisnorhop-17(21)-ene, 22,29,30-trisnorhop-16(17)-ene, Norhopane, 25-norhopene	**1.3** ± 0.4	31	*1.4*	0.94	0.2-1.9
(Poly)aromatics						
Benzene	Benzene	**0.9** ± 0.4	43	*0.8*	1.14	0.4-2.5
Benzaldehyde	Benzaldehyde	**0.6** ± 0.3	41	*0.6*	1.08	0.3-1.5
Acetylbenzene	Acetyl-benzene	**1.1** ± 0.4	39	*1.0*	1.10	0.6-2.3
Alkylbenzenes C3-9	Ethyl-methyl-benzene, Benzene C7, Benzene C9,	**1.9** ± 0.5	23	*1.8*	1.07	1.4-3.5
Polyaromatics	Styrene, Indene, 1,2-dihydro-naphthalene, 2,3-dihydro-inden-1-one, 1-methyl-napthalene, 2methyl-napthalene, Biphenyl, Fluorene, Anthracene	**1.4** ± 0.4	27	*1.3*	1.04	0.8-2.1

955

956

Table 3. Whole-lake and clusters average for a selection of elemental geochemical parameters and of ratios indicative of OM source types and their degradation status

SPECIFIC FEATURES IN GEOCHEMISTRY

	Whole-lake[a]	Near-shore sites	North/East basins	South basin			Shallow central areas
				Shallower	*Intermediate depth*	*Deeper*	
		$Cluster_{geo}$ *4*	$Cluster_{geo}$ *1*	$Cluster_{geo}$ *6*	$Cluster_{geo}$ *2*	$Cluster_{geo}$ *5*	$Cluster_{geo}$ *3*
	(*n*[b]*=42)*	*(n=4)*	*(n=13)*	*(n=10)*	*(n=8)*	*(n=3)*	*(n=4)*
Water depth (m)	**9** ± 7 *(78%)*[c]	**4** ± 2	**5** ± 3	**8** ± 3	**15** ± 4	**24** ± 1	**2** ± 1
Bulk density (g cm^{-3})	**0.06** ± 0.02 *(33%)*	**0.06** ± 0.03	**0.07** ± 0.02	**0.07** ± 0.02	**0.05** ± 0.01	**0.026** ± 0.009	**0.10** ± 0.02
[bSi] (%)	**13** ± 6 *(46%)*	**12** ± 6	**13** ± 3	**15** ± 7	**7** ± 3	**4.2** ± 0.3	**21** ± 4
LOI] (%)	**38** ± 10 *(26%)*	**50** ± 12	**39** ± 5	**34** ± 7	**37** ± 4	**52** ± 2	**20** ± 8
[S] (mg kg^{-1})	**11876** ± 5920 *(50%)*	**17510** ± 833	**11683** ± 3440	**7550** ± 1900	**12896** ± 3315	**26227** ± 4833	**4879** ± 148
[Br] (mg kg^{-1})	**149** ± 35 *(23%)*	**130** ± 6	**153** ± 36	**145** ± 35	**154** ± 19	**204** ± 26	**116** ± 32
[Cu] (mg kg^{-1})	**34** ± 13 *(38%)*	**36** ± 5	**28** ± 6	**30** ± 7	**42** ± 6	**65** ± 10	**24** ± 13
[Ni] (mg kg^{-1})	**19** ± 5 *(25%)*	**21** ± 1	**18** ± 4	**17** ± 2	**21** ± 4	**27** ± 1	**12** ± 4
[Hg] (µg kg^{-1})	**337** ± 202 *(60%)*	**407** ± 141	**251** ± 47	**230** ± 69	**427** ± 94	**917** ± 212	**203** ± 87
[Zn] (mg kg^{-1})	**219** ± 108 *(49%)*	**279** ± 31	**212** ± 68	**139** ± 42	**305** ± 86	**417** ± 33	**63** ± 16
[Fe] (%)	**5** ± 3 *(60%)*	**3.1** ± 2.1	**2.7** ± 1.7	**3.6** ± 1.5	**9.1** ± 2.4	**4.3** ± 2.2	**5.5** ± 1.7
Fe:Al	**1.5** ± 0.8 *(53%)*	**1.0** ± 0.5	**1.0** ± 0.6	**1.1** ± 0.3	***2.5** ± 0.9*	***1.3** ± 0.6*	***1.9** ± 0.3*
[As] (mg kg^{-1})	**35** ± 20 *(57%)*	**27** ± 17	**26** ± 16	**25** ± 11	**64** ± 11	**48** ± 14	**29** ± 9
[P] (mg kg^{-1})	**1624** ± 741 *(46%)*	**927** ± 240	**1065** ± 295	**2088** ± 730	**2074** ± 275	**2766** ± 869	**1224** ± 216
[Mn] (mg kg^{-1})	**729** ± 1690 *(231%)*	**162** ± 53	**182** ± 67	**184** ± 50	**305** ± 93	**171** ± 13	**5700** ± 1597
Mn:Fe	**0.02** ± 0.03 *(150%)*	**0.007** ± 0.002	**0.008** ± 0.003	**0.006** ± 0.002	**0.004** ± 0.001	**0.005** ± 0.002	**0.111** ± 0.051
[Co] (mg kg^{-1})	**19** ± 15 *(79%)*	**15** ± 8	**12** ± 6	**13** ± 5	26 ± 11	**14** ± 2	**49** ± 24
[Pb] (mg kg^{-1})	**192** ± 90 *(47%)*	**199** ± 58	***132** ± 53*	**115** ± 42	**300** ± 59	**315** ± 7	**182** ± 96

SPECIFIC FEATURES IN OM COMPOSITION

		Whole-lake	Near-shore sites	North/East basins	South basin		Shallow central areas	
					Shallower/intermediate depth	*Deeper*		
			$Cluster_{OM}$ *5*	$Cluster_{OM}$ *1*	$Cluster_{OM}$ *3*	$Cluster_{\_OM}$ *2*	$Cluster_{OM}$ *4*	$Cluster_{OM}$ *6*
		(n=42)	*(n=4)*	*(n=16)*	*(n=14)*	*(n=3)*	*(n=3)*	*(n=2)*
Water depth (W.D.)		**9** ± 7 *(78%)*	**4** ± 2	**7** ± 5	**11** ± 5	**24.1** ± 0.5	**3.2** ± 0.9	**1.8** ± 0.1
LOI (%)		**38** ± 10 *(26%)*	**50** ± 12	**39** ± 4	**36** ± 5	**52** ± 2	**24** ± 4	**14** ± 6
(C23-35:0+2K C23-31): Lignins[d]	In-lake:Terrestrial plant OM	**2** ± 1 *(50%)*	**0.8** ± 0.5	**3** ± 1	**1.7** ± 0.4	**1.8** ± 0.6	**3** ± 1	**19** ± 11
N-compounds : Carbohydrates	Algal:Plant OM	**0.37** ± 0.09 *(24%)*	**0.32** ± 0.08	**0.35** ± 0.04	**0**.39 ± 0.05	**0.6** ± 0.1	**0.29** ± 0.02	**0.23** ± 0.05
Chlorophylls : Plant lipids+lignins	Algal:Plant OM	**0.18** ± 0.09 *(50%)*	**0.10** ± 0.05	**0.13** ± 0.06	**0.24** ± 0.08	**0.31** ± 0.07	**0.18** ± 0.05	**0.03** ± 0.03
Proteins:(alkyl)pyrroles+ (alkyl)pyridines+Aromatic N	Algal OM (N-compounds) freshness	**0.3** ± 0.1 *(33%)*	**0.39** ± 0.09	**0.36** ± 0.05	**0.22** ± 0.06	**0.42** ± 0.06	**0.20** ± 0.08	**0.13** ± 0.08
Phytadienes:pristenes[c]	Algal OM (chlorophylls) freshness	**0.4** ± 0.1 *(25%)*	**0.4** ± 0.1	**0.37** ± 0.09	**0.40** ± 0.06	**0.56** ± 0.05	**0.42** ± 0.07	**0.5** ± 0.2
Anhydrosugars:(alkyl)furans & furanones	Plant OM (carbohydrates) freshness	**0.2** ± 0.2 *(100%)*	**0.4** ± 0.2	**0.3** ± 0.2	**0.12** ± 0.11	**0.14** ± 0.04	**0.08** ± 0.01	**0.042** ± 0.002
Guaiacyl-acid:Guaiacyl-aldehyde[e]	Plant OM (lignin) freshness	**0.07** ± 0.03 *(43%)*	**0.13** ± 0.02	**0.07** ± 0.03	**0.05** ± 0.02	**0.04** ± 0.01	**0.04** ± 0.03	**0.10** ± 0.06
Guaiacyl -2C: Guaiacyl -1C[e]	Plant OM (lignin) freshness	**0.8** ± 0.3 *(38%)*	**1.23** ± 0.07	**1.0** ± 0.2	**0.5** ± 0.2	**0.6** ± 0.2	**0.5** ± 0.1	**1.1** ± 0.2
Syringyl-2C:Syringyl-1C[e]	Plant OM (lignin) freshness	**1.0** ± 0.8 *(80%)*	**2.4** ± 0.3	**1.1** ± 0.6	**0.5** ± 0.2	**0.6** ± 0.1	**0.3** ± 0.3	**1.4** ± 0.8

[a] whole-lake: averages of all analyzed sediment samples excluding the two outlier samples (sites M4, S15; cf. Sect. 3.1.1); [b] n: number of samples; [c] the data are presented as follow: **average** ± standard deviation *(relative standard deviation)*; [d] the compounds included in the ratios are given in detail in Table S1 in the supplementary information.

Light grey background denotes average values below whole-lake average (<10%); No background denotes values close to whole-lake average (±10%); Dark grey background are values above whole-lake average (>10%).

Figures

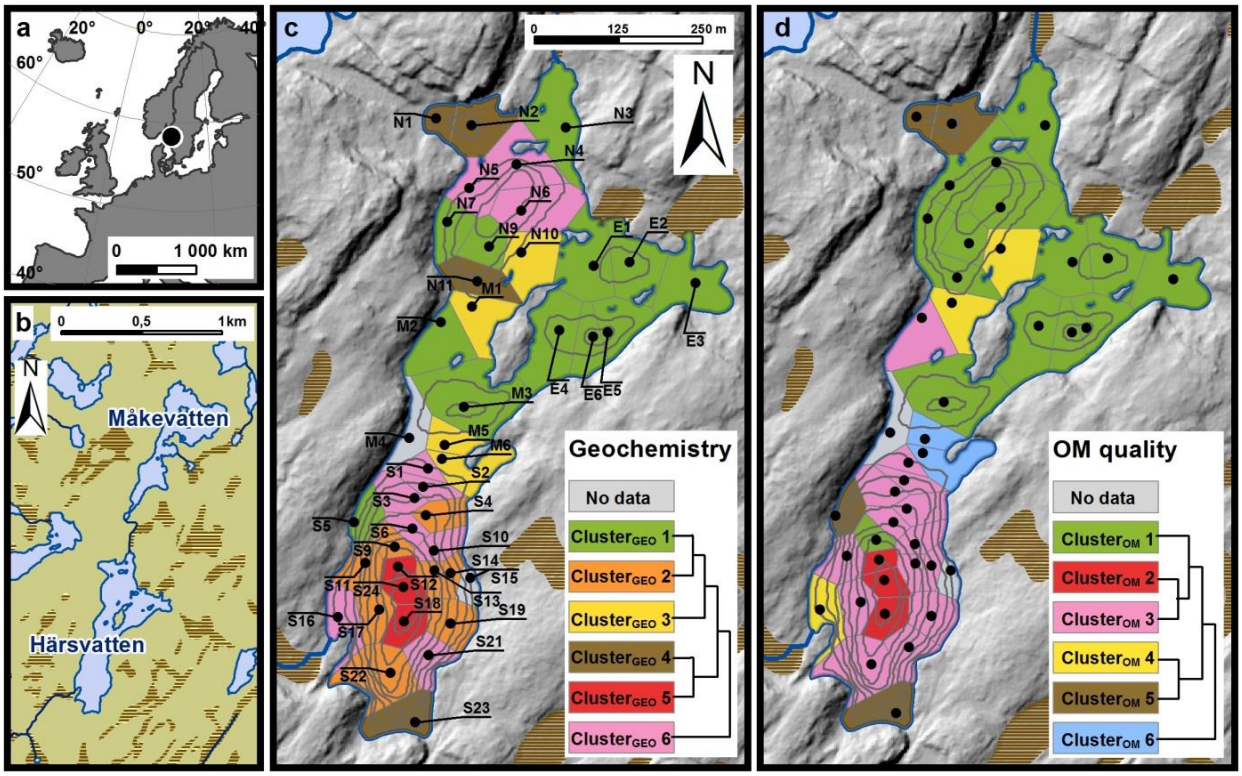

Fig. 1 Maps of Härsvatten showing (a) its location in Europe; (b) its catchment with lakes, mires and larger streams; and (c, d) its bathymetry along with the spatial distribution of the 44 sampling sites and the six selected clusters based on sediment elemental geochemistry (c) and sediment OM molecular composition (d). In the panel c) and d), the dendrogram shows the relationship between the six identified clusters.

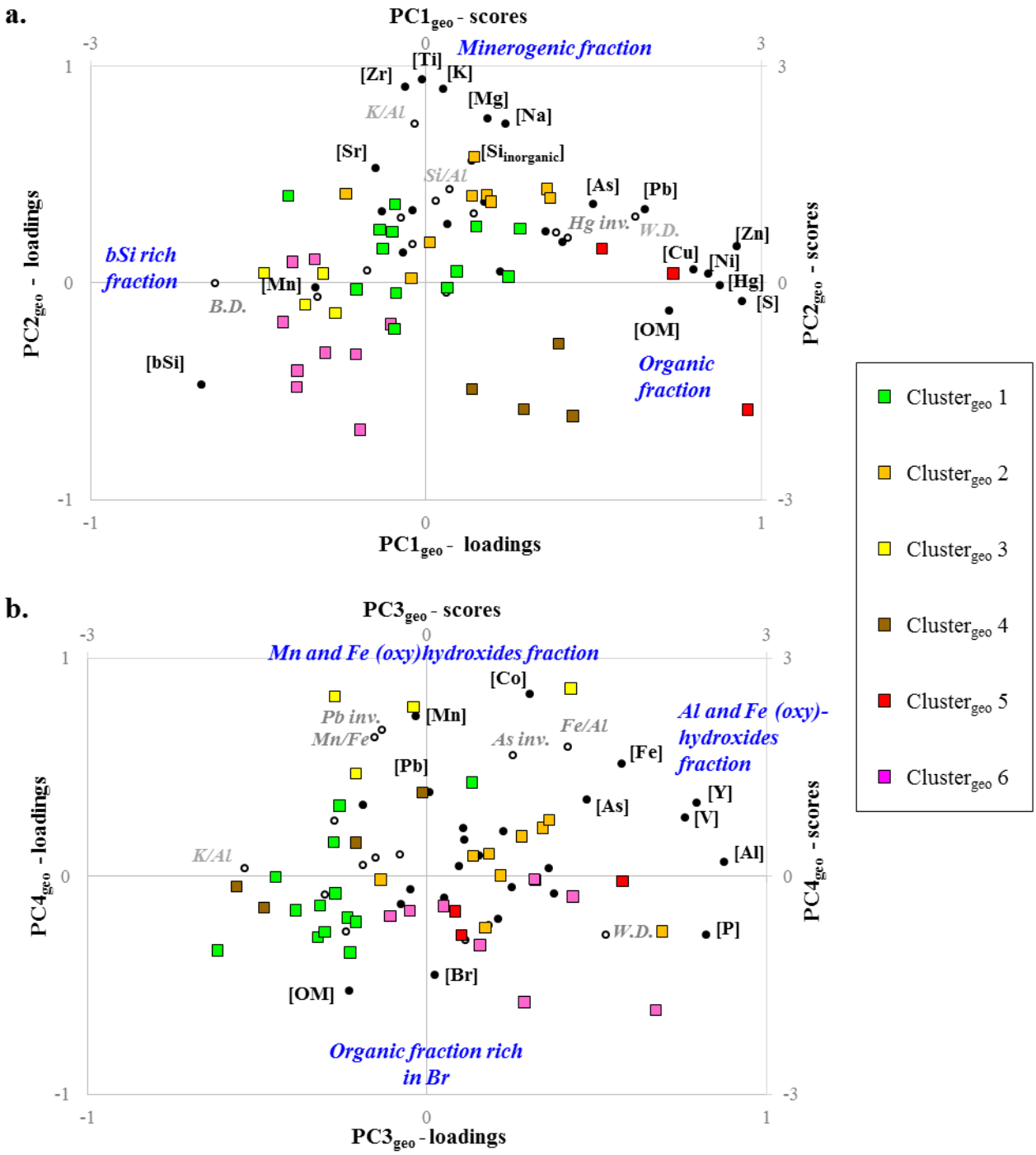

Fig. 2 Combined loading- and score-plots for PCs 1-4 of the elemental geochemistry dataset. For the PC-loadings, filled circles correspond to active variables. Others variables (empty circle and italics letter) were added passively. Sediment samples are colored according to the results of the cluster analysis.

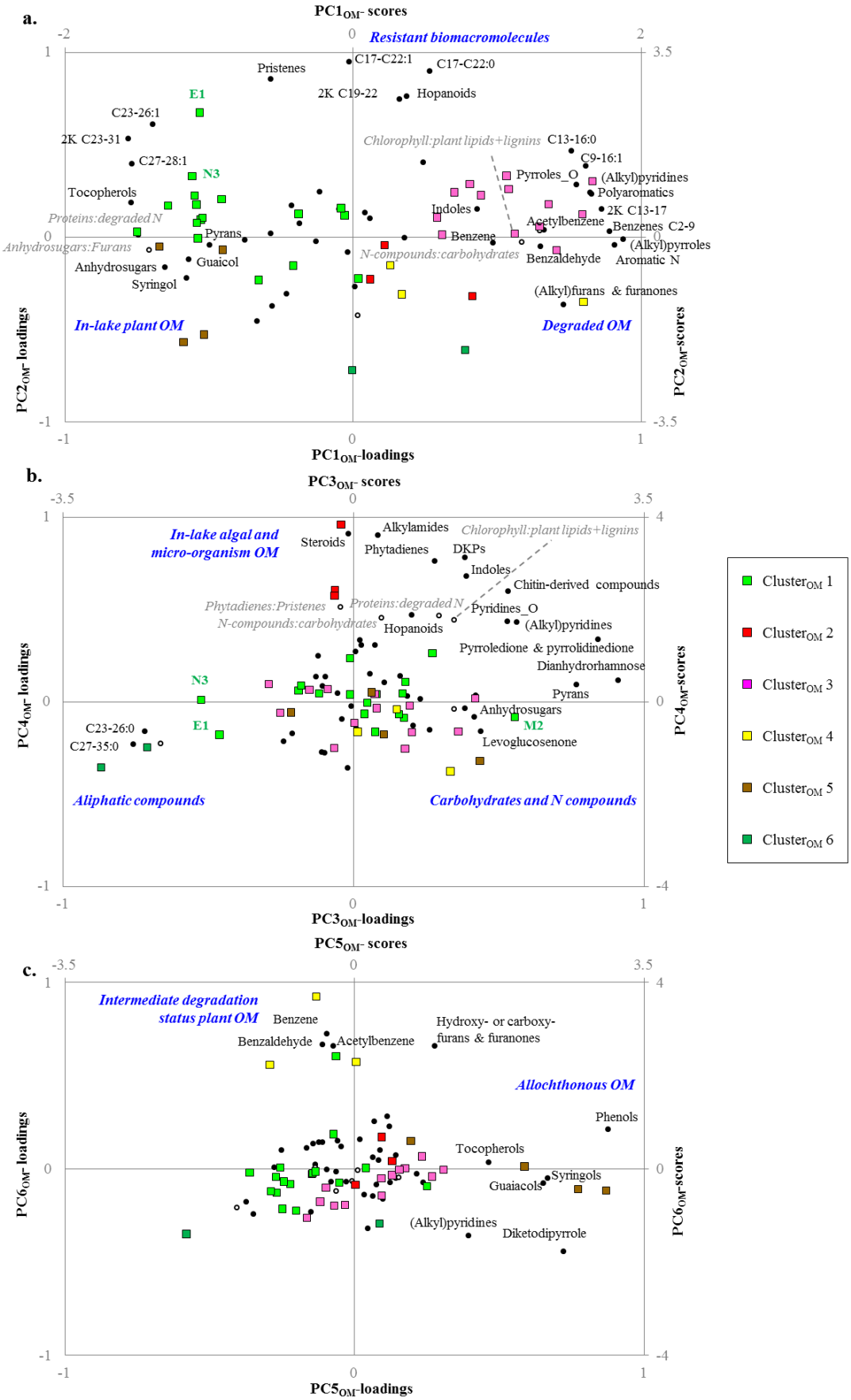

Fig. 3 Combined loading- and score-plots for PCs 1-6 (a, b and c) of the OM molecular composition dataset (i.e. the 41 groups of organic compounds as defined in Table 2). For the PC-loadings, filled circles correspond to active variables. Others variables (empty circle and italics letter) were added passively. Sediment samples are colored according to the results of the cluster analysis.